2010

Intrinsic Features of the Multisensory Cortical Area LRSS in the Ferret

Alexandru Ioan Cojanu
Virginia Commonwealth University

Intrinsic Features of the Multisensory Cortical Area LRSS in the Ferret

By Alexandru Ioan Cojanu, BS

A thesis submitted in partial fulfillment of the requirements for the degree of Master of Science in Anatomy and Neurobiology at the School of Medicine of Virginia Commonwealth University.

Virginia Commonwealth University, 2010.

Major Director: M. Alex Meredith, Ph.D.
Department of Anatomy and Neurobiology

Committee approval date: November 29th, 2010

Acknowledgment

I would like to thank Dr. M. Alex Meredith for his continued guidance and support throughout the duration of this project. I am thankful for the opportunity I had to work in his laboratory and for all his patience and kind words of encouragement for this past year. I would also like to thank Dr. Les Keniston, Dr. Ruth Clemo and Alex Foxworthy for their help and friendship during my time in the laboratory.

I would like to extend my sincere thanks to Dr. George Leichnetz for his constant support and advice over the past two years. I am most grateful to Dr. Mary Shall for her service on my thesis committee.

Most importantly, I would like to express my love and gratitude to my parents, Dr. Daniel N. Cojanu and Dr. Carmen Cojanu for their tireless quest in lovingly guiding and helping me throughout my life. Without their continuous sacrifice, support and inspiration I would have not had the opportunities I had in order to become the man I am today. I love you both and thank you for everything you've done.

Table of Contents

List of Tables

List of Figures

List of Abbreviations

A1= primary auditory cortex
AAF= anterior auditory field
ADF=anterodorsal auditory field
AVF=anteroventral auditory field
AMLS=anteromedial lateral suprasylvian visual field
ALLS=anterolateral lateral suprasylvian visual field
LRSS=lateral rostral suprasylvian sulcal cortex
MRSS=medial rostral suprasylvian sulcal cortex
S1= primary somatosensory cortex
S2=secondary somatosensory cortex
V1=primary visual cortex

Abstract

Intrinsic Features of the Multisensory Cortical Area LRSS in the Ferret

By Alexandru Ioan Cojanu, BS

A thesis submitted in partial fulfillment of the requirements for the degree of Master of Science in Anatomy and Neurobiology at the School of Medicine of Virginia Commonwealth University.

Virginia Commonwealth University, 2010.

Major Director: M. Alex Meredith, Ph.D.
Department of Anatomy and Neurobiology

Environmental events simultaneously transduced by more than one sensory modality underlie multisensory processing in the CNS. While most studies of multisensory processing examine functional effects, none have evaluated the influence of local or columnar circuitry. The goal of the present study is to examine of local features of the ferret lateral rostral suprasylvian sulcus (LRSS), a multisensory cortex. Immunostaining revealed the cytoarchitectonic features of the LRSS: thick supragranular layers, a narrow layer IV, and moderately stained but differentiated infragranular layers. Golgi-Cox techniques were used with light microscopy and digital reconstruction to document neuronal morphology. Among the 90 reconstructed neurons, 4 distinct forms or pyramidal and 2 types of non-pyramidal neurons were found. Measurement of maximal dendritic spread indicates that a cortical column in the LRSS was 250.9 um in diameter. These results describe local features of the LRSS upon which future experiments of intrinsic circuitry will be based.

INTRODUCTION

It is well established that events in the surrounding environment are transduced by specific sensory receptors and relayed to the central nervous system (CNS) for processing that ultimately produces perception and behavior. For the most part, these sensory information streams have been largely regarded as separate pathways emanating from different sensory receptors and are sensory modality-specific. For example, sensory information from the skin, eye, or ear reaches the primary sensory cortices which are arranged into distinct areas representing the somatosensory, visual and auditory modalities. A great deal is known regarding the organization and function of these primary sensory areas in a variety of animal models. However, because an environmental event can be simultaneously transduced, or sensed, by more than one sensory modality, the nervous system must deal with the processing of multiple sensory inputs at the same time. This means that information flow from different sensory systems must converge on individual neurons at some point in the central nervous system, creating what is now known as multisensory convergence. This convergence of inputs onto individual neurons creates a condition where a certain sensory modality is influenced by the presence of one or more sensory modalities unlike the primary one. A great example of this is the ventriloquist effect (Howard and Templeton, 1966) where subjects are provided a visual stimulus (in the form of a puppet held by an entertainer) and an auditory stimulus (the voice of the entertainer). The effect comes into play when the entertainer has the ability to throw his voice, without obvious movements of his

mouth (which would provide visual stimuli to the audience) so it appears to come from the puppet, whose mouth is moved by the entertainer (the actual visual stimuli). In doing so, the audience perceives the auditory stimuli (entertainer's voice) to be coming from the same place as the visual stimuli (the puppet), when in fact they do not originate in the same place. Many other examples of such multisensory processing exist such as the cocktail party effect (Sams et al., 1991), the McGurk effect (McGurk and MacDonald, 1976) and cross-modal matching (Stein and Meredith, 1993), among others.

The organization and function of the pathways underlying this and other types of multisensory processing are far less understood than those of unisensory processing streams (for example auditory alone or visual alone). Although many non-primary areas of sensory cortex have long been regarded as 'polysensory' or 'associational' (between the different senses), there have been very few studies that examined their organizational and connectional features as they relate to their multisensory functions.

One example of such a study is that of the superior temporal sulcal (STS) region of the primate cortex which has been long identified as a multisensory region (Benevento et al., 1977; Leinonen et al., 1980; Bruce et al.1981; Schroeder and Foxe, 2002; Smiley, 2007; Ghazanfar, 2005; Ghazanfar, 2008) where convergence of visual and auditory inputs predominates. In this area alone, four distinct areas of multisensory convergence have been identified (TPO 1-4). Recent studies have indicated that this convergence underlies the processing and enhancement of the auditory components of speech when visual inputs from lip movements are activated (McGurk, 1976; Sams et al., 1991; Calvert et al., 2000; Jääskeläinen, 2010). The inputs from other cortical areas underlying

this phenomenon have also been identified (Selzer and Pandya, 1982). Furthermore, the cytoarchitecture and neuronal morphology of the STS has been described (Elston, 2001).

Another example of an area that expresses multisensory convergence is the superior colliculus, a structure common to many animals and vastly studied in the cat. The superior colliculus is found in the midbrain and has been shown to mediate attention and behavior. The neurons in this particular structure respond to visual, auditory and somatosensory stimuli, with the overlapping receptive fields of each of these sensory modalities serving to screen the information that ultimately reaches its circuitry and integrative fields (Stein and Meredith, 1993). Each modality (visual, auditory, somatosensory) has its own map-like representation. These maps are in topographical register with one another and are primarily constituted of multisensory neurons, with each individual multisensory neuron containing receptive fields for each modality represented. It has been shown that concurrent arrival of inputs from more than one sensory modality onto such multisensory neurons in the superior colliculus leads to altered patterns of neural activity and response. Behavioral tests in cats show an enhanced detection and orientation to a visual stimulus when it is combined with an auditory stimulus and a decreased detection and orientation to a visual stimulus when it was presented with an auditory stimulus at a different location.

It is now also well established that cortical activity is the product of the integration of extrinsic inputs with local processing. Recently, there has been an explosion of information regarding local processing with the invention of *in vitro* slice physiology techniques coupled with intracellular labeling and caged-glutamate release (Callaway and Katz, 1993). In contrast, due to the unviability of mature primate tissue

(at its expense) in this type of preparation, no studies of intrinsic connectivity of multisensory cortex have been reported.

Cortical tissue from adult ferrets, unlike that of adult monkeys, is viable in slice preparations (Meredith lab, preliminary data), but there are few studies that identify multisensory regions of the ferret brain. These limited studies have designated the medial and lateral banks of the ferret suprasylvian sulcus (MRSS and LRSS) (Keniston, 2009; Keniston, 2008), Area 21 (Allman, 2008), the pseudosylvian sulcal cortex (PSSC) (Ramsay and Meredith, 2003) and auditory areas posterior pseudosylvian field (PPF), posterior suprasylvian sulcus (PSF), primary auditory cortex (AI), anterior auditory field (AAF), anterior dorsal field (ADF) and anterior ventral field (AVF) (Bizley and King, 2009; Bizley and King, 2008; Bizley, 2007) as having multisensory properties.

Of these ferret multisensory cortical regions, perhaps the best studied and most intensely multisensory area is that of the LRSS, an area dividing the primary somatosensory cortex (SI) medially (Rice et al., 1993) from four (AVF, ADF, AAF and AI) distinct auditory areas laterally (Bizley et al., 2005; Kowalski et al., 1995) and bordered caudally by the visual anteriolateral lateral suprasylvian (ALLS) area (Homman-Ludiye et al., 2010). A recent functional study of the LRSS (Keniston et al., 2008) sought to examine the multisensory properties of the area by means of recording *in vivo* responses to controlled, repeated auditory, somatosensory and combined auditory-somatosensory stimuli, therefore identifying neurons that responded to only one sensory modality (defined as unimodal), neurons that responded to more than one sensory modality (defined as a bimodal form of multisensory neuron), and those which responded to only one sensory modality, but that response was significantly modulated by the

presence of a stimulus from a second modality (termed subthreshold multisensory neuron). The study demonstrated that the LRSS contains a large population (62% of total neuronal sample) of multisensory neurons. These multisensory neurons reported as bimodal (46% of total neuronal population) and subthreshold multisensory (16% of total neuronal population). Furthermore, anatomical tracers established that the LRSS received inputs from somatosensory cortical areas SI and MRSS as well as from auditory cortical areas A1 and AAF. Thus, in the context of cortical activity, the LRSS's multisensory function is matched by connectional features of its extrinsic inputs. However, nothing is known of the region's local circuitry and how these critical functions contribute to multisensory processing. Therefore, the present study was conducted in order evaluate the components and potential connectivity of local circuits in the LRSS.

Before conducting *in vitro* slice experiments on the LRSS, it is essential to understand the region's cytoarchitecture and the morphology of its neuronal components. Being part of the neocortex (also known as the isocortex), it is expected that the LRSS would exhibit the characteristic six-layered laminar pattern described by Mountcastle (1998). These layers, referred to by their roman numerals, include, in sequence from outside to inside: layer I, known as the plexiform or molecular layer containing horizontally running axons and dendrites; layer II, known as the external granular layer, containing small pyramidal cells in addition to a number of nonpyramidal cells; the external pyramidal layer (layer III) containing medium-sized pyramidal cells with many nonspiny, nonpyramidal cells; the internal granular layer (layer IV) containing many small neurons tightly packed; layer V, known as the internal pyramidal layer containing

large pyramidal cells; and layer VI, the multiform or spindle layer containing cells of varying morphology.

However, within that broad framework, there are many variations of neuronal and fiber-tract patterns (e.g., Brodmann Areas), and these variations also occur in the size and exact location of cytoarchitectonic areas not only between different brains, but also between the hemispheres of the same brain (Mountcastle, 1998). The present study used a well-established immunohistochemistry neuronal marker (SMI-32) to assess the cytoarchitecture of the LRSS region, a technique previously used in describing the ferret MRSS (Keniston, 2009), the descending projections to the ferret inferior colliculus (Bajo, 2007) and the subdivisions of the cat primary auditory areas (Mellot, 2010) among others. Next, to examine the neuronal morphology of the LRSS region, the Golgi method of neuronal staining was used. This procedure is based on the staining principles described by Ramon-Moliner (1970) which showed complete neuronal somata and dendritic labeling. The procedure itself stains approximately 10% of the total neuronal population, however the mechanism by which this technique works is still largely unknown. Numerous studies have used the Golgi-Cox technique in order to analyze the morphological properties of neurons (Chen et al., 2009; Furtak et al., 2007; Faherty et al., 2003 and Prieto et al., 1999) including the seminal works of Ramon-y-Cajal (1899).

In summary, the goal of the present study was to document the cytoarchitectonics and morphological properties of constituent neurons of a robust multisensory area in an animal model conducive for further exploration using in vitro slice techniques.

MATERIALS AND METHODS

Animal and Tissue Preparation

Young, adult male ferrets (n=3) of ages between 118-137 days old (avg. age=130 days old) and weights between 1.3-1.6 kg (avg. weight=1.4 kg) were used in the present study (see Table 1). The animals were anesthetized with an intraperitoneal injection of 60 mg/kg of sodium pentobarbital and, once becoming areflexive, they were perfused transcardially with 0.9% saline followed by 0.4% paraformaldehyde. All procedures were conducted with the approval of the Animal Care and Use Committee of Virginia Commonwealth University and in accord with the National Research Council's *Guidelines for the Care and Use of Mammals in Neuroscience and Behavioral Research (2003)* concerning the responsible use of animals in research. Following the perfusion, the cortex of both hemispheres was stereotaxically blocked in the coronal plane into 7-10 mm thick segments. These were then prepared for staining using the FD Rapid Golgi Stain Kit (FD Neurotechnologies, Ellicott City, MD, USA). The tissues were rinsed briefly in double-distilled water and then immersed in a Golgi-Cox solution containing 5% potassium dichromate, 5% mercuric chloride and 5% potassium chromate in double distilled water. This mixture was replaced once after the first 24 hours and then stored at room temperature in the dark for 14 days. After this initial immersion period, the blocks of tissue were transferred to "Solution C" (FD Rapid Golgi Stain Kit), stored and incubated in the dark for 7 days. A vibratome was then used to section the tissue blocks serially at 100µm thickness in the coronal plane following which the sections were transferred to gelatin-coated glass microscope slides. Transferred sections were coated

with additional “Solution C” with the excess being removed by filter paper. These mounted sections were then left to dry in a humidor at room temperature overnight. After drying, the mounted sections were rinsed with double distilled water and reacted in equal parts of “Solution D” (FD Rapid Golgi Stain Kit) and “Solution E” (FD Rapid Golgi Stain Kit) in the dark for 10 minutes. These sections were then rinsed in double distilled water for 4 minutes and dehydrated with 50%, 75% and 100% ethanol, cleared in xylene and finally coverslipped with Permount (Fisher Scientific, Fair Lawn, NJ). The finished slides were archived for later analysis.

TABLE 1. Animal characteristics.

	Ferret 1	Ferret 2	Ferret 3	Average
Age (days)	137	118	136	130
Weight (kg)	1.3	1.3	1.6	1.4
Sex	male	male	male	male

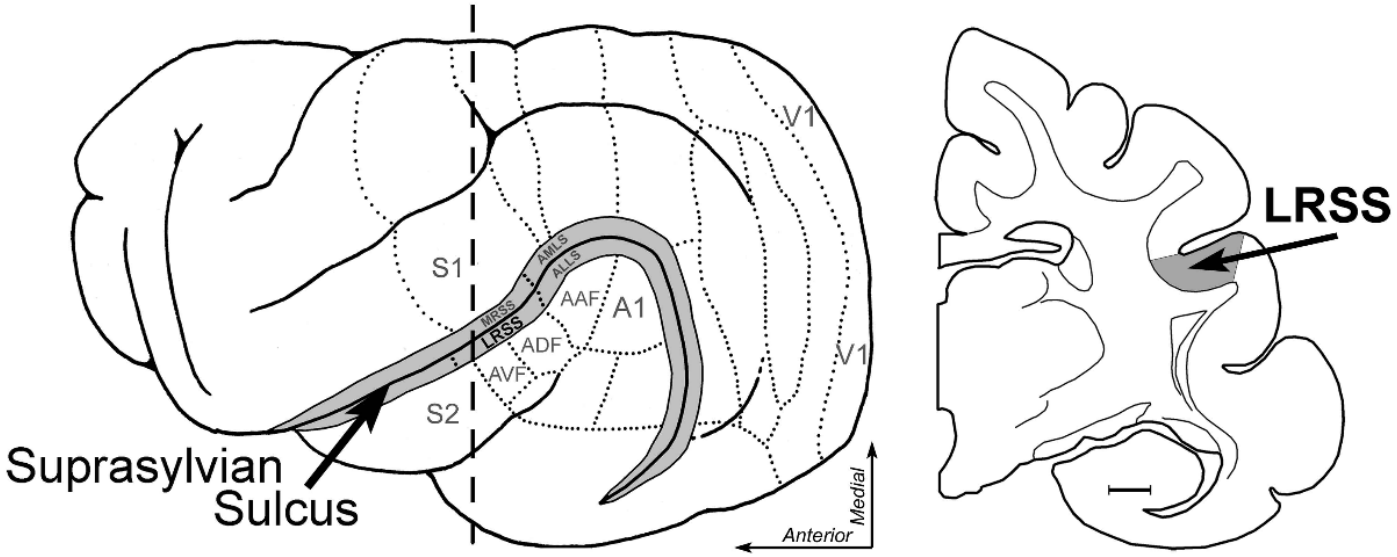

Figure 1. Location of the ferret LRSS. Depicted on the left is a lateral view of the ferret left cerebral cortex, with its sulci and gyri. The suprasylvian sulcus (arrow) is opened and colored gray. Dotted lines indicate the borders of known sensory representations. The dashed vertical line corresponds to the location from which the coronal section, on right, is taken. On the coronal section, the area in the bank of the lateral suprasylvian sulcus colored grey is the LRSS (at arrow). A1= primary auditory cortex; AAF= anterior auditory field; ADF=anterodorsal auditory field; AVF=anteroventral auditory field: AMLS=anteromedial lateral suprasylvian visual field; ALLS=anterolateral lateral syprasylvian visual field; LRSS=lateral rostral suprasylvian sulcal cortex; MRSS=medial rostral suprasylvian sulcal cortex; S1= primary somatosensory cortex; S2=secondary somatosensory cortex; V1=primary visual cortex.

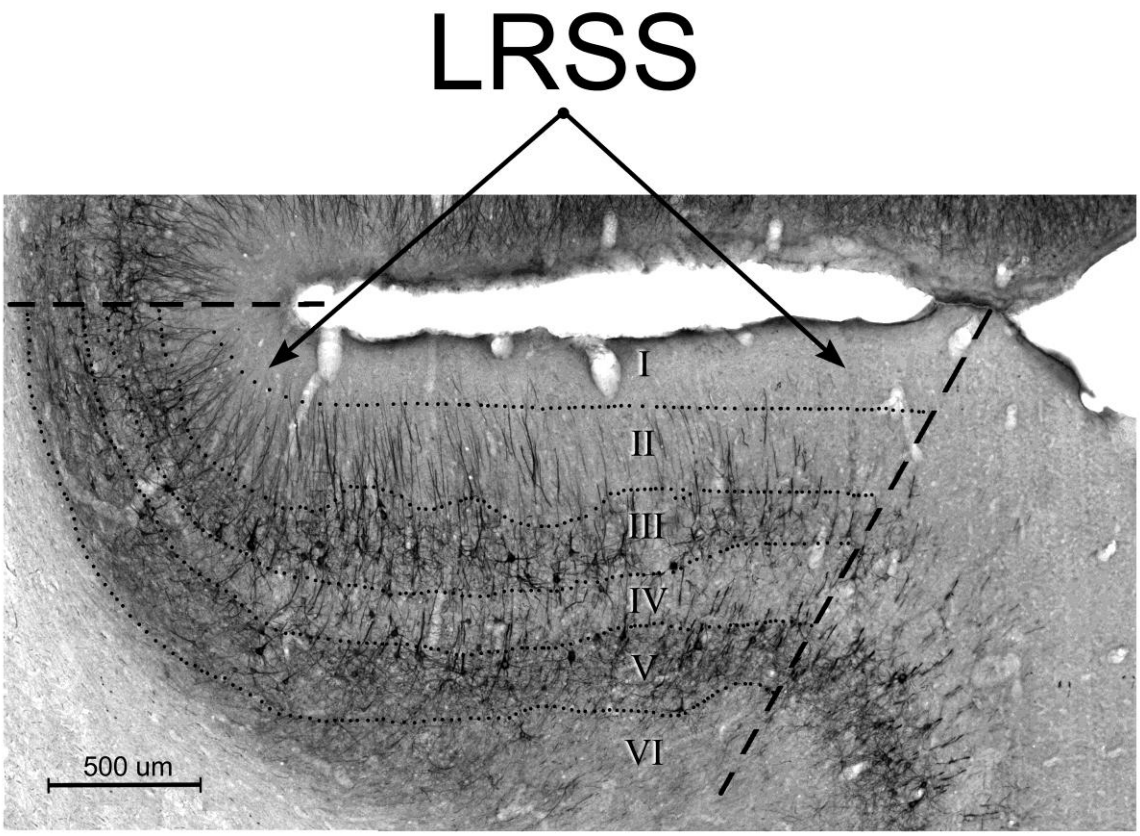

Figure 2. The laminar organization of the LRSS. This coronal section was immunocytochemically stained using the antibody SMI-32 to show the cytoarchitecture of the region. The lateral bank of the suprasylvian sulcus is depicted and the LRSS is located between the dashed lines at arrows. The LRSS shows the typical neocortical lamination consisting of 6 layers (roman numerals) numbered from I (near the pial surface) to VI (at bottom near the grey-white border). Note the presence of well-stained pyramidal neurons and dendritic processes in layers III and V. Scale bar = 500 um

Identification, selection and reconstruction of sample neurons

The goal of this study was to examine the morphology of neurons in a cortical area that processes multisensory information. The selected region, the Lateral Rostral Suprasylvian Sulcal (LRSS) region, meets this multisensory criterion (Keniston et al., 2009). Golgi-Cox stained sections containing the LRSS were surveyed using low magnification light-microscopy to identify candidate neurons for tracing and reconstruction. Candidate LRSS neurons were required to display adequate Golgi-Cox labeling of their soma and connected dendrites and only those with limited staining artifacts were chosen for tracing. Once a candidate LRSS neuron was found, the entire brain section in which it was located was traced using a light microscope and Neurolucida software (MBF Bioscience, MicroBrightField, Williston, VT, USA). Important features of the section that were traced at low magnification (4x) included the outline, the grey-white border and ventricles, if present. Subsequent tracing of the neuronal somata and dendritic branches were done at higher (400x) magnification. This process was repeated for different neurons and different tissue sections until an adequate and representative number of neurons were collected from each animal.

Once the entire sample of LRSS neurons had been traced, features of their morphology were subsequently analyzed with the Neuroexplorer (MBF Bioscience, MicroBrightField, Williston, VT, USA) software. The laminar location (1-6 layers) of the cell body was identified and recorded for each neuron. In addition, a total of 24 measurements were made of each neuron's somatic and dendritic characteristics. The specific measurements that were performed on each traced neurons included the following somatic parameters: 1) Somatic perimeter (μm); 2) Somatic Area (μm^2);

3) Feret Max (the longest diameter of the soma); 4) Feret Min (the longest diameter perpendicular to the feret max); 5) Aspect ratio (calculated as "aspect = feret max/feret min" and being indicative of the symmetric shape shown by a soma). The dendritic parameters measured for each individual neuron were: 1) Quantity of basilar dendrites; 2) Quantity of basilar dendritic nodes, including bifurcating and trifurcating nodes; 3) Total length of basilar dendrites (µm); 4) Mean length of basilar dendrites (µm); 4) Total surface area of basilar dendrites (µm^2); 5) Mean surface area of basilar dendrites (µm^2); 6) Total volume of basilar dendrites (µm^3); 7) Mean volume of basilar dendrites (µm^3); 8) Quantity of apical dendrite nodes, including bifurcating and trifurcating nodes; 9) Maximum horizontal spread of basilar dendrites in the lateral direction (µm); 10) Maximum horizontal spread of basilar dendrites in the medial direction (µm); 11) Total maximum horizontal spread of basilar dendrites (µm) measured by summing the basilar horizontal spread from the lateral and medial directions; 12) Total length of apical dendrite (µm); 13) Total surface area of the apical dendrite (µm^2); 14) Total volume of the apical dendrite (µm^3); 15) Distance from soma to first apical branch point (µm); 16) Maximum horizontal spread of the apical dendrite in the lateral direction (µm); 17) Maximum horizontal spread of the apical dendrite in the medial direction (µm); 18) Total apical horizontal spread (µm) measured by summing the apical horizontal spread in the lateral and medial directions. The neuronal features that were measured are summarized in Table 2.

After the compilation of these 24 descriptive neuronal characteristics, statistical methods were used to determine the average and standard deviation of the various measurements. The data was then tabulated according to each neuron's laminar

location and a distribution of means for each feature was generated using Microsoft Excel (Microsoft Corp.). These manipulations revealed, for some features, a clustering of values that permitted the segregation of neuron features into 6 distinct categories: Layer II pyramidal neurons with bifurcating apical dendrites; Layer II pyramidal neurons with nonbifurcating apical dendrites; Layer III pyramidal neurons; Layer V-VI pyramidal neurons; Layer II-III nonpyramidal neurons; Layer V-VI nonpyramidal neurons, as summarized in Table 3. Finally, images of neurons and their scales, reconstructed in the NeuroExplorer software (MBF Bioscience, MicroBrightField, Williston, VT, USA) were imported into Adobe Photoshop (Adobe Systems) for graphic manipulation and display.

TABLE 2. Neuronal morphological features analyzed

Table 2. Morphological Parameters of Neurons That Were Analyzed With Neurolucida and Neurolucida Explorer

Somatic Variables	Basilar Dendrites	Apical Dendrite		Maximal Horizontal Spread (µm)
Perimeter (µm)	Quantity			Lateral apical dendrite (µm)
Area(µm^2)	Nodes	Nodes	Distance from soma to first apical branch point (µm)	Medial apical dendrite (µm)
Feret Max(µm)	Length (µm)	Length (µm)		Total apical spread (µm)
Feret Min(µm)	Mean Length (µm)	Surface area (µm^2)		Lateral basilar dendrite (µm)
Aspect	Surface area (µm^2)	Volume (µm^3)		Medial basilar dendrite (µm)
	Mean Surface area (µm^2)			Total basilar spread (µm)
	Volume (µm^3)			
	Mean Volume (µm^3)			

TABLE 3. Designation of neurons per group.

	Ferret 1	Ferret 2	Ferret 3	total # neurons per group
Layer II pyramidal with bifurcating apical dendrite	5	6	3	14
Layer II pyramidal neuron nonbirfurcating apical dendrite	3	1	3	7
Layer III pyramidal neurons	11	12	9	32
Layer V-VI pyramidal neurons	3	6	1	10
Layer II-III nonpyramidal neurons	5	1	6	12
Layer V-VI nonpyramidal neurons	6	7	2	15
Total # neurons	33	33	24	90

RESULTS

Classification of neurons based on morphological characteristics

The multisensory LRSS region is found in the bank of the Suprasylvian Sulcus (Fig. 1) and it varies in thickness between ~750um – 2000 um. The region contains the typical six cortical layers associated with the neocortex as described by Mountcastle (Mountcastle, 1998). A total of 90 Golgi-Cox stained LRSS neurons from 3 animals (see Table 3) were reconstructed and measured. The main criteria by which neurons were distinguished into morphologically distinct categories was whether they were pyramidal neurons or not, as described by Feldman (Feldman, 1984). Following this initial distinction, the neurons were further split into categories based on the cortical layer they were found in and other specific morphological characteristics. The morphological features of each of the six distinct groups of neurons were evaluated as follows and are summarized in Appendix 1.

Group 1: Layer II pyramidal neurons with bifurcating apical dendrite

All neurons (n=14, 15.5%) in this group had cell bodies located in Layer II with apical dendrites extending into Layer I, often to the pial surface. Furthermore, the apical dendrite exhibited a clear bifurcation, where the daughter branches were essentially the same thickness or caliber, usually within 25 µm of the soma (the distance from soma to the first apical branch point was avg=21.9 µm; stdev= 14.4 µm; all data are reported as average and standard deviation). A typical Group 1 neuron is illustrated in Figure 16.

In terms of somatic characteristics, Group 1 neurons exhibited common somatic perimeters (avg=55.2 µm; stdev=5.9 µm), somatic area (avg=202.7 µm²; stdev=31.3 µm²), high values for feret max (avg=19.8 µm; stdev=2.4), feret min (13.6 µm; stdev=1.0 µm), and high aspect ratio (avg=1.5; stdev=0.2).

Apical dendrites exhibited the largest length (avg=1278.7µm; stdev = 592.4 µm), largest number of nodes for the apical dendrite (avg=12.9; stdev=6.7), largest apical dendrite surface area (avg=5050.7 µm²; stdev=2288.0 µm²) and largest volume of apical dendrites (avg=2073.4 µm³; stdev=995.4 µm³) out of the four pyramidal neuron groups.

Other common features of Group 1 are the number of basilar dendrites (avg=3.1; stdev=1.2), number of nodes found in the basilar dendrites (avg=11.4; stdev=7.5), total length of basilar dendrites (avg=1033.0 µm; stdev=516.3 µm), mean length of individual basilar dendrites (avg=344.9 µm; stdev=136.6 µm), surface area of basilar dendrites (avg=3085.5 µm²; stdev=1421.3 µm²), mean surface area of individual basilar dendrites (1026.4 µm²; stdev=375.3 µm²), volume of basilar dendrites (avg=918.9 µm³; stdev=453.7 µm³) and mean volume of individual basilar dendrites (303.5 µm³; 126.0 µm³).

In addition, Group 1 neurons displayed large total apical dendrite maximum horizontal spread (avg=207.4 µm; stdev=71.6 µm), calculated by summing the horizontal spread of the medial aspect of the apical dendrite (avg=94.9 µm; stdev=46.5 µm) and the horizontal spread of the lateral aspect of the apical dendrite (avg=112.6 µm; stdev=41.8 µm). The total maximum horizontal spread of Group 1 neurons' basilar dendrites (avg=201.6 µm; stdev=61.7 µm) was also calculated by summing the horizontal spread of the medial aspect of the basilar dendrites (avg=93.0 µm; stdev=32.5 µm) and the

horizontal spread of the lateral aspect of the basilar dendrites (avg=108.5 µm; stdev=52.6 µm). These data are summarized in Appendix A, Table A1.

Group 2: Layer II pyramidal neurons with nonbifurcating apical dendrite

Figure 17 represents examples of neurons from the second morphological group, Group 2 (n=7; 7.8% of total neuronal population), which exhibited a single apical dendrite that often extended to the pial surface. These neurons had their first apical branch (avg=25.7 µm; stdev=10.0 µm) on average 3.8 µm farther than those of Group 1 (Group 2 avg=25.7 µm; Group 1 avg=21.9 µm). Group 2 neurons, however, had smaller somatic perimeter (avg=52.1 µm; stdev=5.9 µm), somatic area (avg=183.1 µm^2; stdev=35.8 µm^2), feret max (avg=18.7 µm; stdev=2.5 µm), feret min (avg=13.3 µm; stdev=1.4 µm) and aspect ratio (avg=1.4; stdev=0.1) than did Group 1 neurons.

These neurons also had fewer total apical nodes (avg=9.6; stdev=3.3), a smaller average apical dendrite length (avg=1041.2 µm; stdev=362.4 µm), smaller apical dendrite surface area (avg=3735.4 µm^2; stdev=1236.6 µm^2) and smaller apical dendrite volume (avg=1404.1 µm^3; stdev=482.5 µm^3).

Group 2 neurons also exhibited a smaller number of basilar dendrites (avg=2.7; stdev=0.8) and smaller number of nodes (avg=11.3; stdev=3.7) than their layer II, Group 1 counterparts. However, they had larger values of the total length of basilar dendrites (avg=1093.4 µm; stdev=298.82 µm), mean length of individual basilar dendrites (avg=426.5 µm; stdev=158.3 µm), surface area of basilar dendrites (avg=3200.4 µm^2; stdev=936.7 µm^2), mean surface area of individual basilar dendrites (avg=1248.9 µm^2;

stdev=461.9 μm²), volume of basilar dendrites (avg=975.0 μm³; stdev=417.9 μm³) and mean volume of individual basilar dendrites (avg=380.1 μm³; stdev=184.4 μm³).

Values for the horizontal spread of Group 2 pyramidal neurons showed smaller total apical dendrite maximum horizontal spread (avg=183.5 μm; stdev=47.1 μm), calculated by summing the horizontal spread of the medial aspect of the apical dendrite (avg=92.9 μm; stdev=19.2 μm) and the horizontal spread of the lateral aspect of the apical dendrite (avg=90.5 μm; stdev=40.1 μm). However, Group 2 neurons had larger total maximum horizontal spread of basilar dendrites (avg=250.9 μm; stdev=68.7 μm), calculated by summing the horizontal spread of the medial aspect of the basilar dendrites (avg=102.6 μm; stdev=16.3 μm) and the horizontal spread of the lateral aspect of the basilar dendrites (avg=148.3 μm; stdev=59.0 μm). These values are summarized in Appendix A, Table A2.

Group 3: Layer III pyramidal neurons

Group 3 neurons (n=32; 35.6% of total neuronal population) are characterized by being Layer III pyramidal neurons (Figure 18) of the multisensory LRSS region. Their apical dendrites project vertically through Layer II and Layer I and branch (distance from the soma to the first apical branch avg=26.4 μm; stdev=23.1 μm) farthest away from the soma out of all the groups. Noticeable characteristics, shown in Appendix A, Table A3, include the somatic perimeter (avg=56.1 μm; stdev=7.5 μm), somatic area (avg=200.8 μm²; stdev=41.8 μm²), feret max (avg=18.5 μm; stdev=2.1 μm), feret min (avg=14.5 μm; stdev=1.7 μm) and aspect ratio (avg=1.3; stdev=0.1).

Group 3 neurons have the smallest number of apical dendrite nodes (avg=9.2; stdev=4.2), apical dendrite length (avg=884.0 µm; stdev=399.3 µm), apical dendrite surface area (avg=3319.6 µm²; stdev=1709.5 µm²) and apical dendrite volume (avg=1435.0 µm³; stdev=902.1 µm³).

Other significant characteristics displayed by Group 3 neurons were number of basilar dendrites (avg=4.0; stdev=1.2), number of basilar dendrites nodes (avg=11.2; stdev=5.4), total length of basilar dendrites (avg=1045.4 µm; stdev=596.7 µm), mean length of individual basilar dendrites (avg=261.3 µm; stdev=129.3 µm), surface area of basilar dendrites (avg=3155.3 µm²; stdev=1825.2 µm²), mean surface area of individual basilar dendrites (avg=776.8 µm²; stdev=349.8 µm²), total volume of basilar dendrites (avg=997.8 µm³; stdev=648.1 µm³) and mean volume of individual basilar dendrites (avg=244.0 µm³; stdev=123.7 µm³).

These cells also exhibited the smallest total apical dendrite maximum horizontal spread (avg=175.7 µm; stdev=80.6 µm) as compared with the other groups of pyramidal neurons (Groups 1, 2, and 4). This measure was calculated by summing the horizontal spread of the medial aspect of the apical dendrite (avg=89.5 µm; stdev=59.0 µm) and the horizontal spread of the lateral aspect of the apical dendrite (avg=86.3 µm; stdev=39.8 µm). The total maximum horizontal spread of basilar dendrites (avg=228.8 µm; stdev=72.5 µm) was the second largest out of the five pyramidal neuron groups. This measure was calculated by summing the horizontal spread of the medial aspect of the basilar dendrites (avg=109.2 µm; stdev=44.6 µm) and the horizontal spread of the lateral aspect of the basilar dendrites (avg=117.4 µm; stdev=48.9 µm).

Group 4: Layer V-VI pyramidal neurons

Figure 19 depicts representative cells from Group 4 (n=10; 11.1% of total neuronal population). These are pyramidal in nature, have a single apical dendrite that extends vertically towards the pia from which the first branches occur close to the soma (distance from the soma to the first apical branch avg=10.5 µm; stdev=6.1 µm). The apical dendrite of these cells extends through Layer IV and into Layer III but not farther. Group 4 neurons exhibit the largest somatic perimeter size (avg=56.1 µm; stdev=5.9 µm), somatic area (avg=206.9 µm²; stdev=34.1 µm²) and feret max (avg=19.8 µm; stdev=3.0 µm) out of all groups analyzed. Also of notice are their feret min (avg=14.5 µm; stdev=0.8 µm) and somatic aspect ratio (avg=1.4; stdev=0.2).

The apical dendrite characteristics were not impressive, ranking third out of the four pyramidal groups in the number of apical dendrite nodes (avg=9.8; stdev=3.2); they also exhibited the smallest apical dendrite length (avg=1038.1 µm; stdev=429.0 µm), apical dendrite surface area (avg=3217.0 µm²; stdev=1163.4 µm²); and had the smallest apical dendrite volume (avg=1065.1 µm³; stdev=373.1 µm³) of the pyramidal groups.

Other common features of Group 4 neurons were the number of basilar dendrites (avg=3.8; stdev=1.7), total number of basilar dendrite nodes (avg=10.9, stdev=7.3), total basilar dendrite length (avg=1011.8 µm; stdev=655.9 µm), mean length of individual basilar dendrites (avg=258.8 µm; stdev=157.5 µm),), surface area of basilar dendrites (avg=3116.8 µm²; stdev=1752.7 µm²), mean surface area of individual basilar dendrites (avg=807.9 µm²; stdev=391.6 µm²), total volume of basilar dendrites (avg=948.8 µm³; stdev=484.5 µm³) and mean volume of individual basilar dendrites (avg=250.9 µm³; stdev=111.4 µm³).

Compared with the other three pyramidal neuron groups, Group 4 neurons had the largest total apical dendrite maximum horizontal spread (avg=211.0 µm; stdev=131.6 µm), as measured by summing the horizontal spread of the medial aspect of the apical dendrite (avg=115.8 µm; stdev=120.6 µm) and the horizontal spread of the lateral aspect of the apical dendrite (avg=95.1 µm; stdev=34.5 µm). However, they ranked third in terms of the value for the total maximum horizontal spread of basilar dendrites (avg=226.6 µm; stdev=88.8 µm) as calculated by summing the horizontal spread of the medial aspect of the basilar dendrites (avg=109.2 µm; stdev=44.6 µm) and the horizontal spread of the lateral aspect of the basilar dendrites (avg=117.4 µm; stdev=48.9 µm). These results are summarized in Appendix A, Table A4.

Table 4. Somatic characteristics: Groups 1-6.

		SOMATIC VARIABLES				
		Perimeter(μm)	Area(μm²)	Feret Max(μm)	Feret Min(μm)	Aspect Ratio
Neuron Group						
Layer II pyramidal with bifurcating apical	avg	55.2	202.7	19.8	13.6	1.5
	stdev	5.9	31.3	2.4	1.0	0.2
Layer II pyramidal nonbifurcating apical	avg	52.1	183.1	18.7	13.3	1.4
	stdev	5.5	35.8	2.5	1.4	0.1
Layer III pyramidal neurons	avg	56.1	200.8	18.5	14.5	1.3
	stdev	7.5	41.8	2.1	1.7	0.1
Layer V-VI pyramidal neurons	avg	56.1	206.9	19.8	14.5	1.4
	stdev	5.9	34.1	3.0	0.8	0.2
Layer II-III nonpyramidal neurons	avg	51.8	160.0	17.0	12.5	1.4
	stdev	14.5	38.7	2.9	1.9	0.2
Layer V-VI nonpyramidal neurons	avg	55.7	202.3	19.7	13.5	1.5
	stdev	8.7	58.2	3.5	2.0	0.3

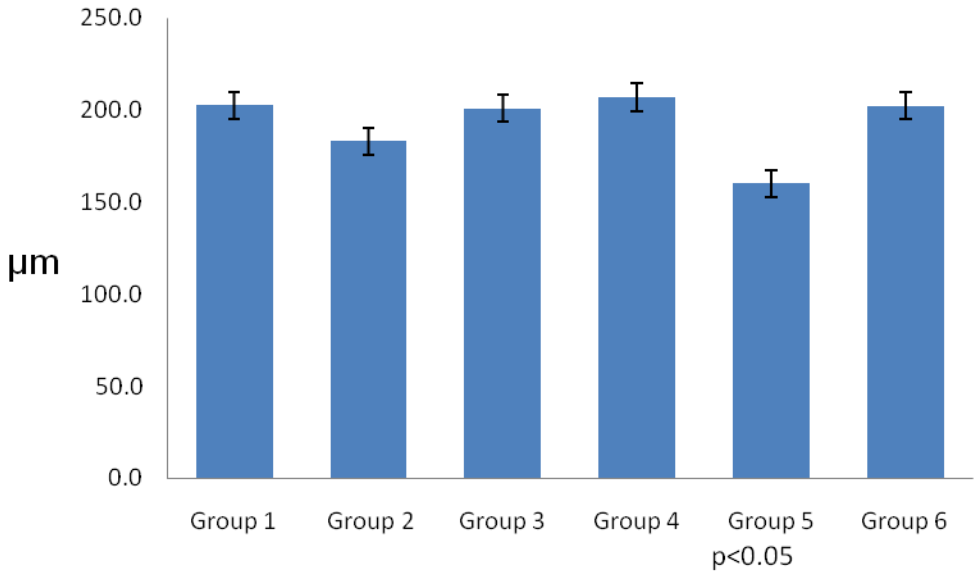

Figure 3. Somatic perimeter characteristics: Groups 1-6

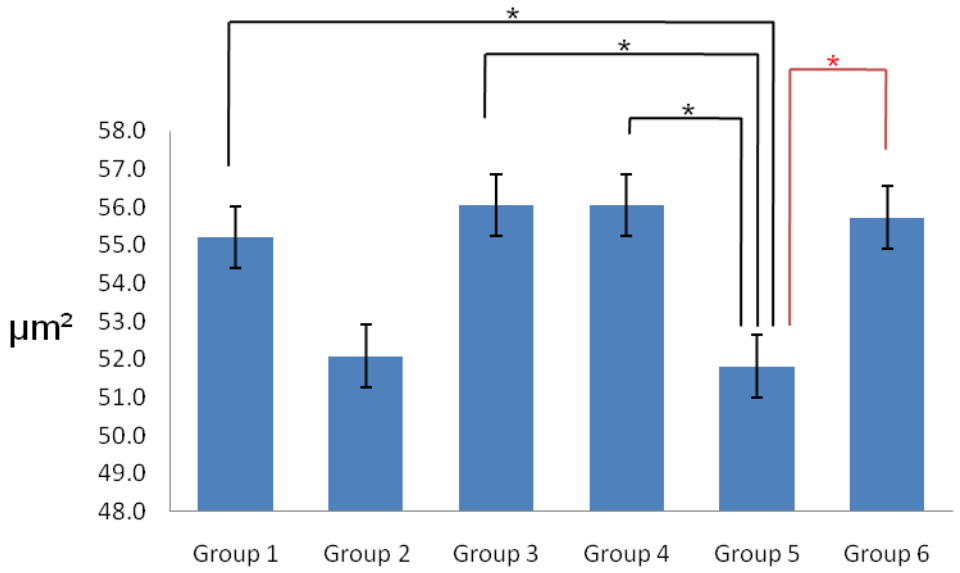

Figure 4. Somatic area characteristics: Groups 1-6

Table 5. Dendritic characteristics: pyramidal Groups 1-4.

		BASILAR DENDRITES								Apical Dendrite			
Neuron Group		Qty	Nodes	Length(µm)	mean len	Surface(µm²)	mean sur	Volume(µm³)	mean vol	Nodes	Length(µm)	Surface(µm²)	Volume(µm³)
Layer II pyramidal with bifurcating apical	avg	3.1	11.4	1033.0	344.9	3085.5	1026.4	918.9	303.5	12.9	1278.7	5050.7	2073.4
	stdev	1.2	7.5	516.3	136.6	1421.3	375.3	453.7	126.0	6.7	592.4	2288.0	995.4
Layer II pyramidal nonbifurcating apical	avg	2.7	11.3	1093.4	426.5	3200.4	1248.9	975.0	380.1	9.6	1041.2	3735.4	1404.1
	stdev	0.8	3.7	298.8	158.3	936.7	461.9	417.9	184.4	3.3	362.4	1236.6	482.5
Layer III pyramidal neurons	avg	4.0	11.2	1045.4	261.3	3155.3	776.8	997.8	244.0	9.2	884.0	3319.6	1435.0
	stdev	1.2	5.4	596.7	129.3	1825.2	349.8	648.1	123.7	4.2	399.3	1709.5	902.1
Layer V-VI pyramidal neurons	avg	3.8	10.9	1011.8	258.8	3116.8	807.9	948.8	250.9	9.8	1038.1	3217.0	1065.1
	stdev	1.7	7.3	655.9	157.5	1752.7	391.6	484.5	111.4	3.2	429.0	1163.4	373.1

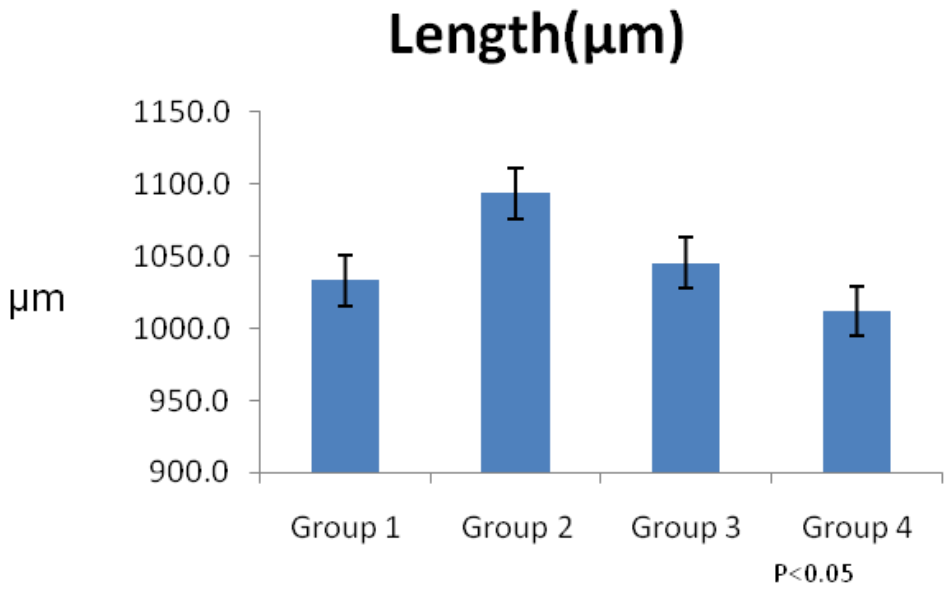

Figure 5. Basilar dendrite length: Groups 1-4.

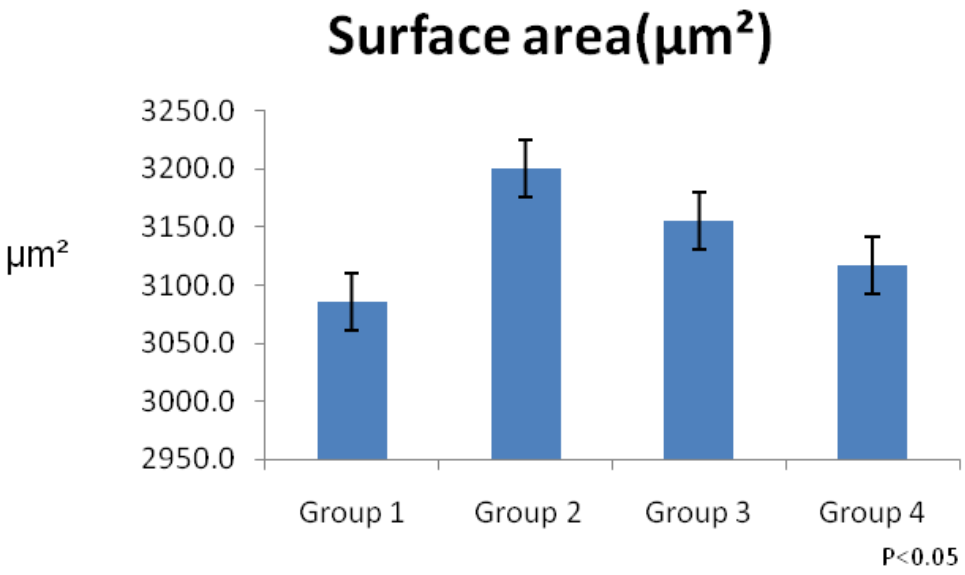

Figure 6. Basilar dendrite surface area: Groups 1-4.

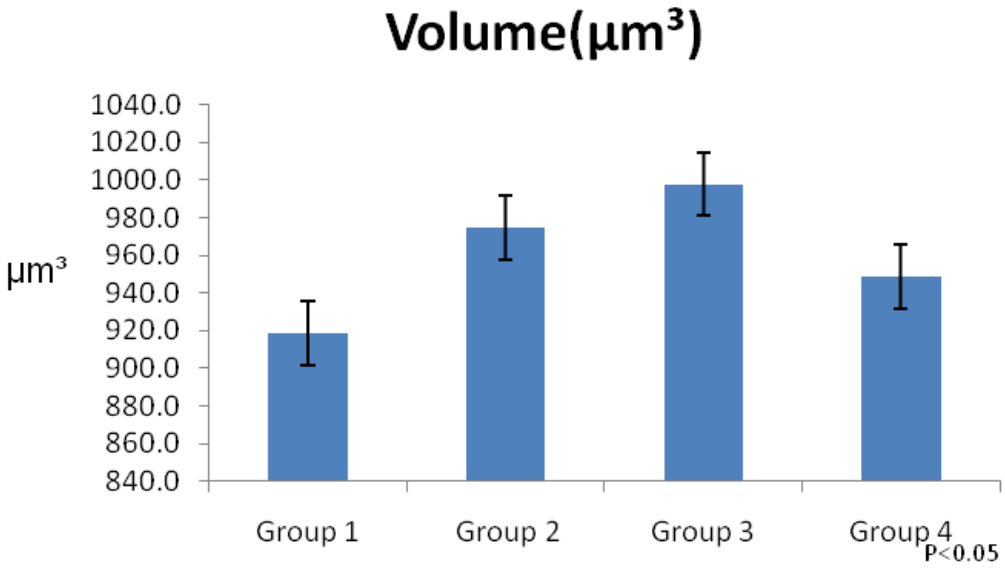

Figure 7. Basilar dendrite volume: Groups 1-4.

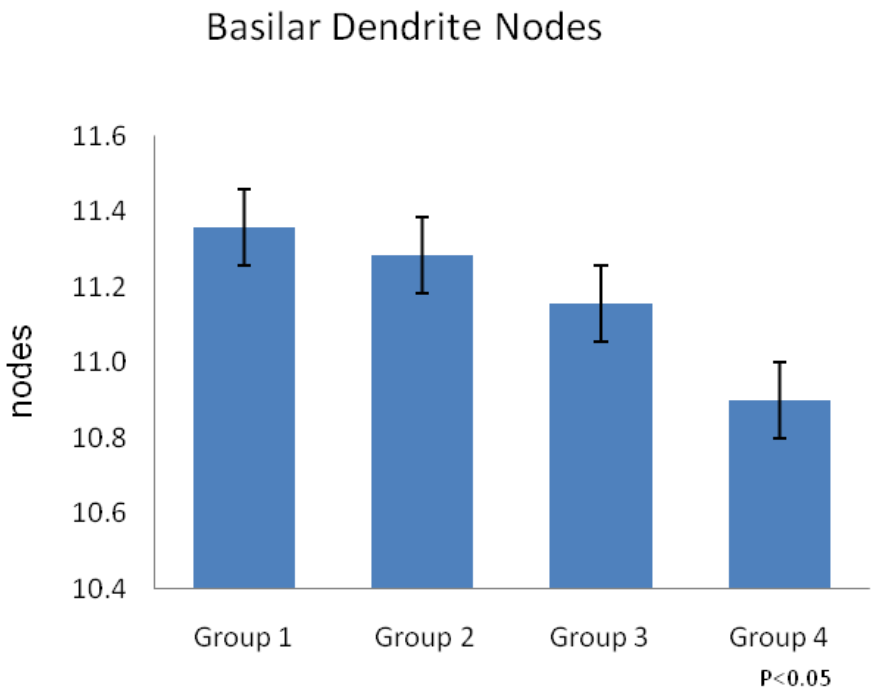

Figure 8. Basilar dendrite nodes: Groups 1-4.

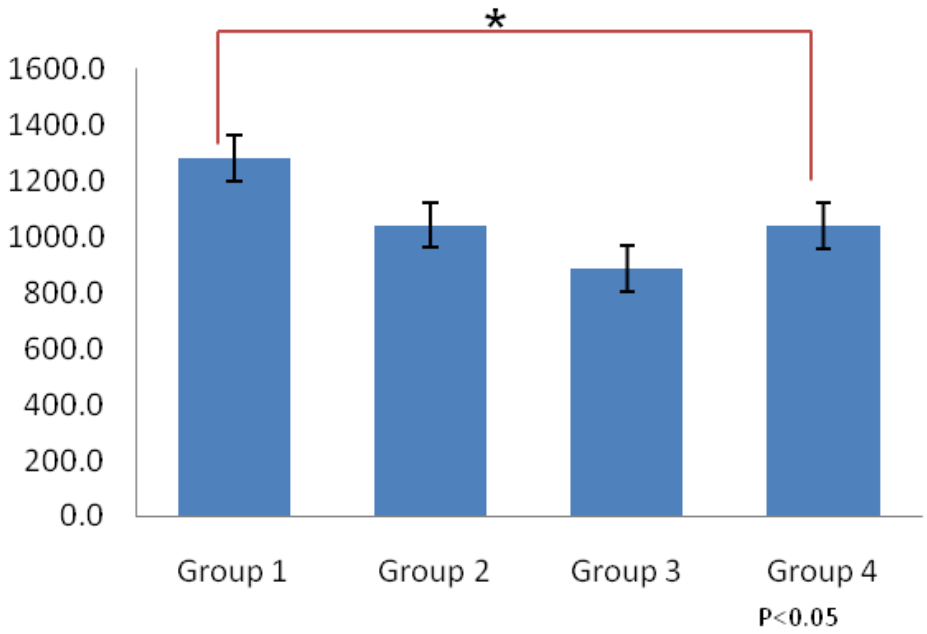

Figure 9. Apical dendrite length: Groups 1-4.

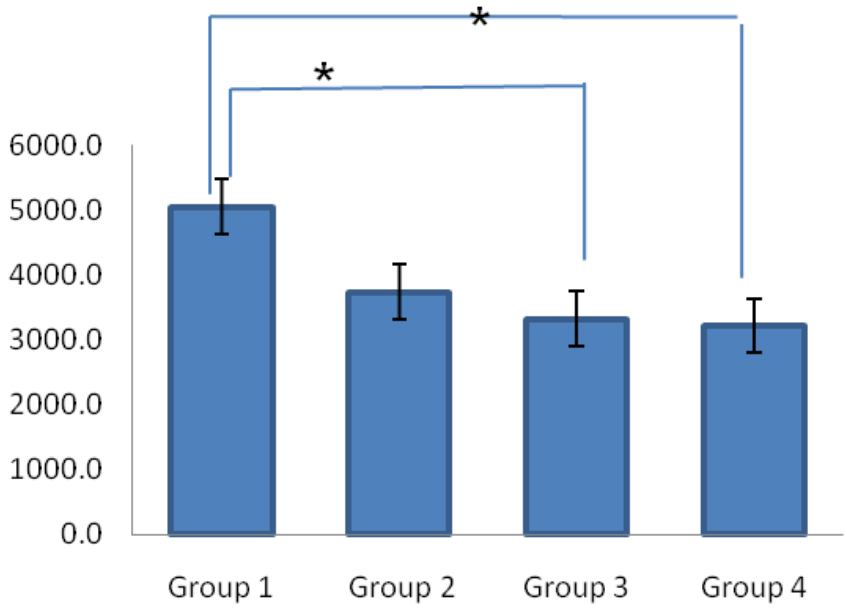

Figure 10. Apical dendrite surface area: Groups 1-4.

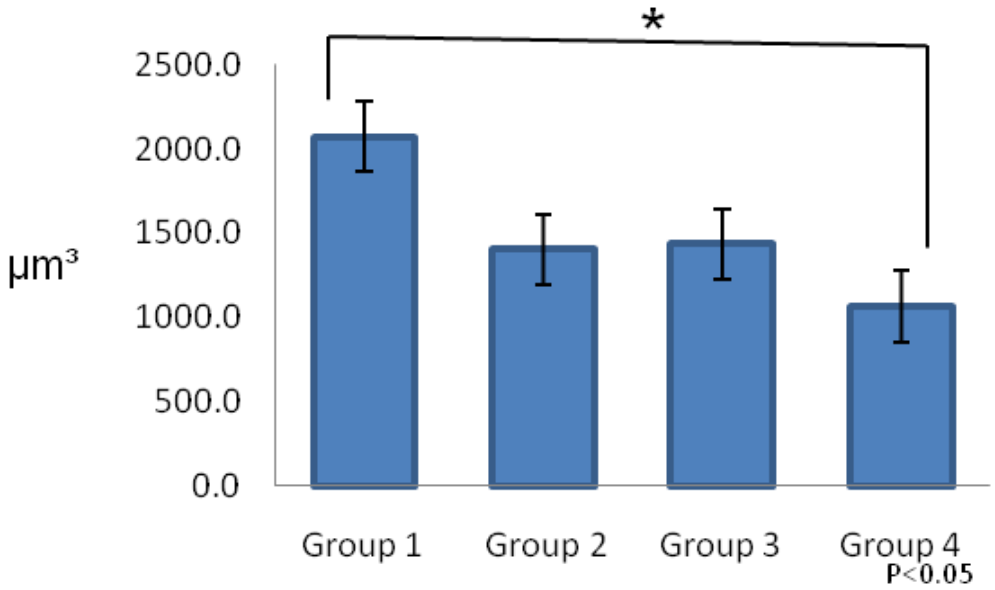

Figure 11. Apical dendrite volume: Groups 1-4.

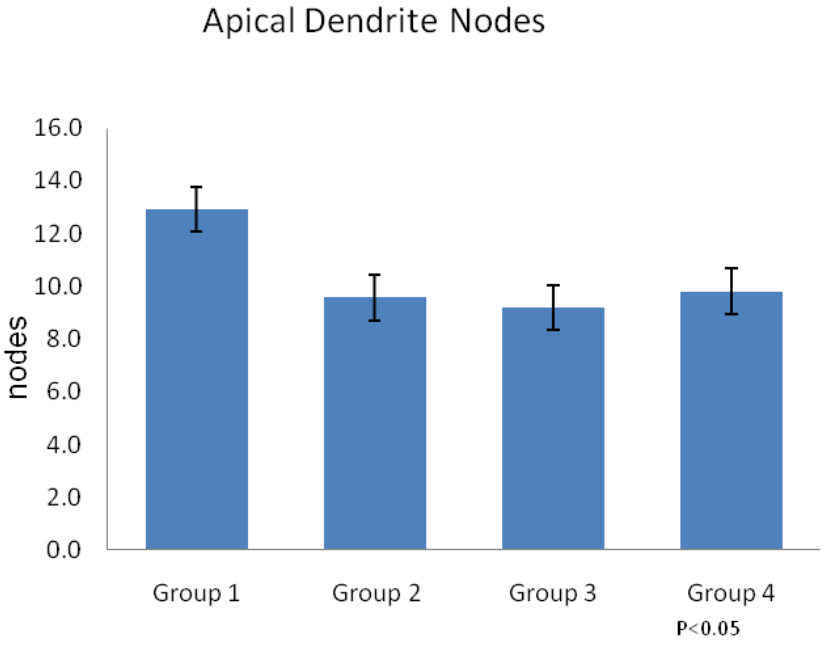

Figure 12. Apical dendrite nodes: Groups 1-4.

Table 6. Maximum horizontal spread: pyramidal Groups 1-4

Neuron Group		MAXIMUM HORIZONTAL SPREAD (µm)						Distance from soma to first apical branch point (µm)
		APICAL DENDRITE			BASILAR DENDRITES			
		medial	lateral	total apical	medial	lateral	total basilar	
Layer II pyramidal with bifurcating apical	avg	94.9	112.6	207.4	93.0	108.5	201.6	21.9
	stdev	46.5	41.8	71.6	32.5	52.6	61.7	14.4
Layer II pyramidal nonbifurcating apical	avg	92.9	90.5	183.5	102.6	148.3	250.9	25.7
	stdev	19.2	40.1	47.1	16.3	59.0	68.7	10.0
Layer III pyramidal neurons	avg	89.5	86.3	175.7	121.2	107.6	228.8	26.4
	stdev	59.0	39.8	80.6	59.3	50.2	86.9	23.1
Layer V-VI pyramidal neurons	avg	115.8	95.1	211.0	109.2	117.4	226.6	10.5
	stdev	120.6	34.5	131.6	44.6	48.9	88.8	6.1

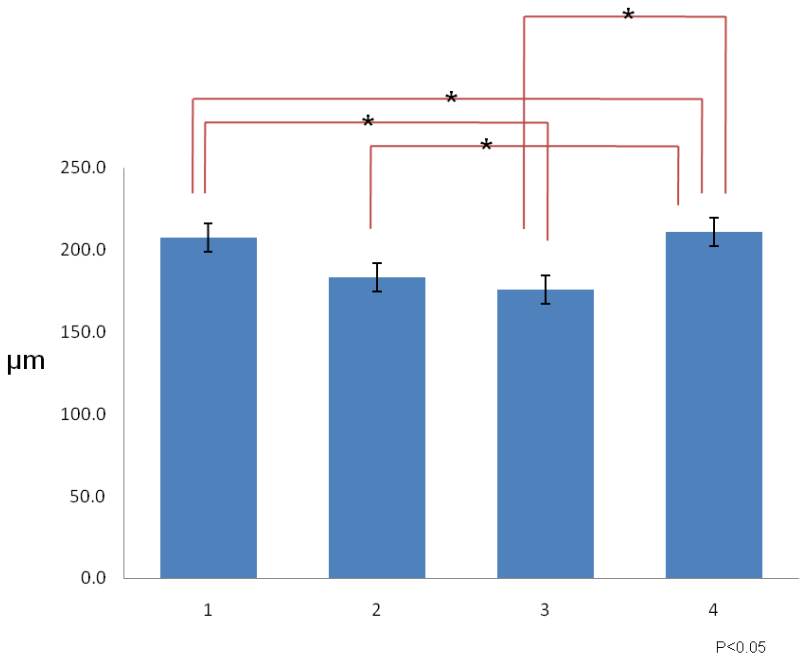

Figure 13. Maximum apical dendrite horizontal spread: Groups 1-4.

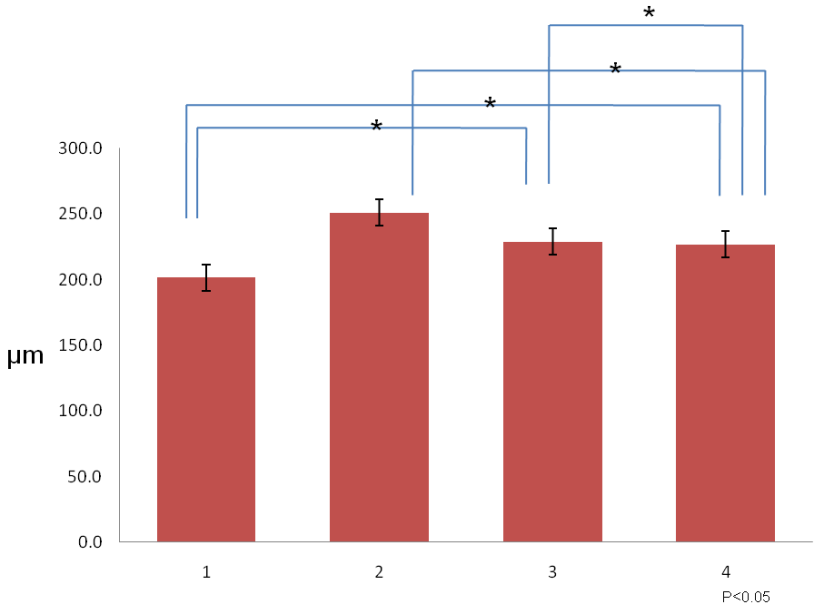

Figure 14. Maximum basilar dendrite horizontal spread: Groups 1-4.

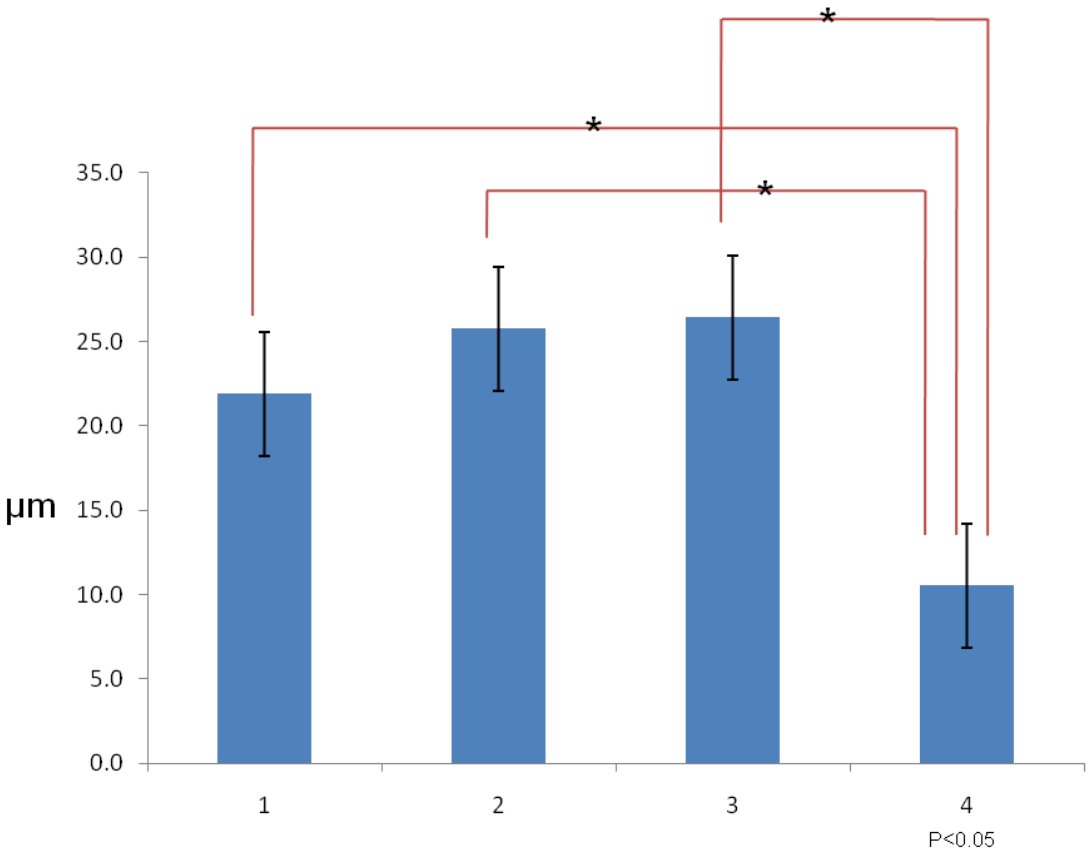

Figure 15. Distance from soma to first apical branch point: Groups 1-4.

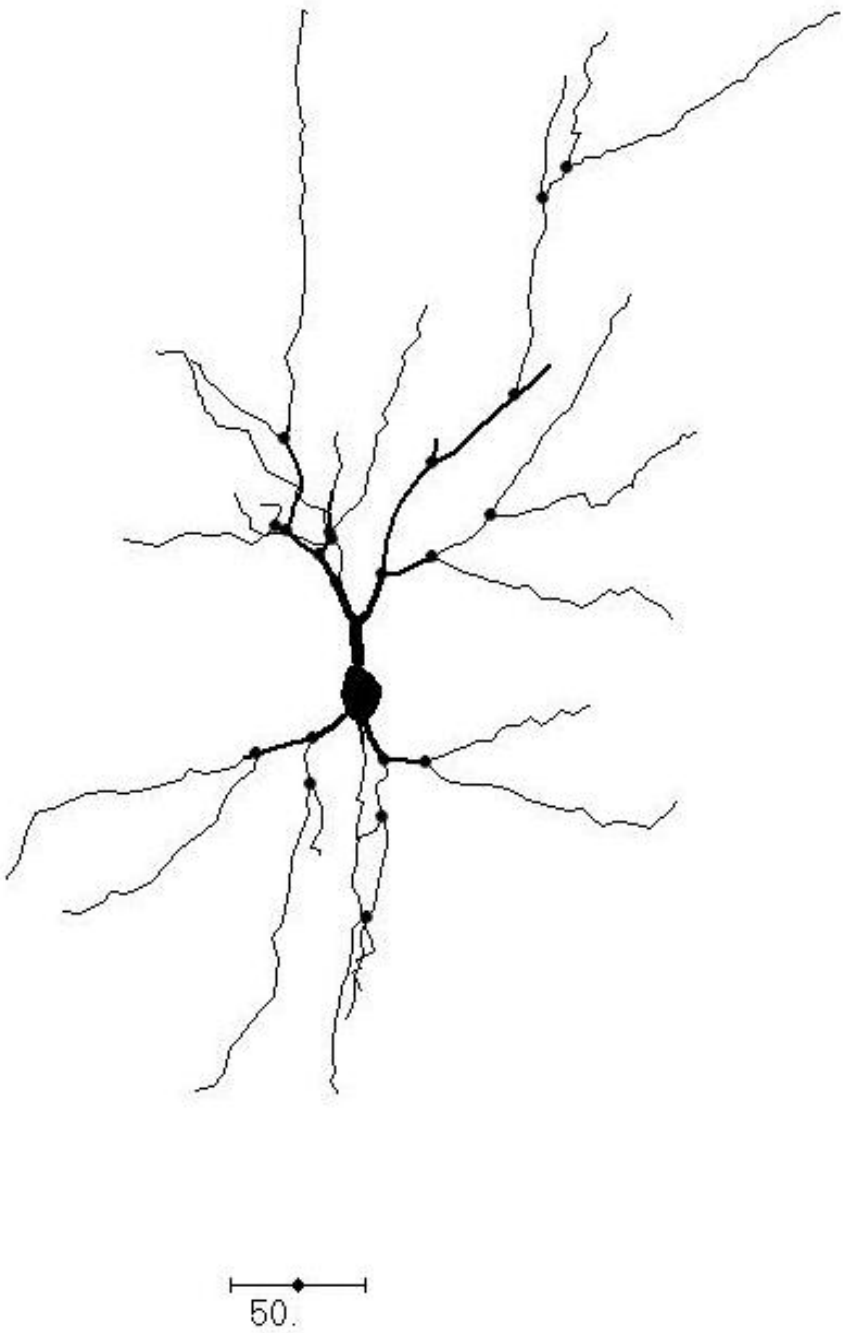

Figure 16. Neuron of Group 1. These layer II pyramidal neurons (n=14 neurons) exhibited a clear bifurcation at an average of 21.9 µm from the soma, where the daughter branches were essentially the same thickness. Cells are oriented so that the pia is at the top of the page. Scale bar: 50 µm.

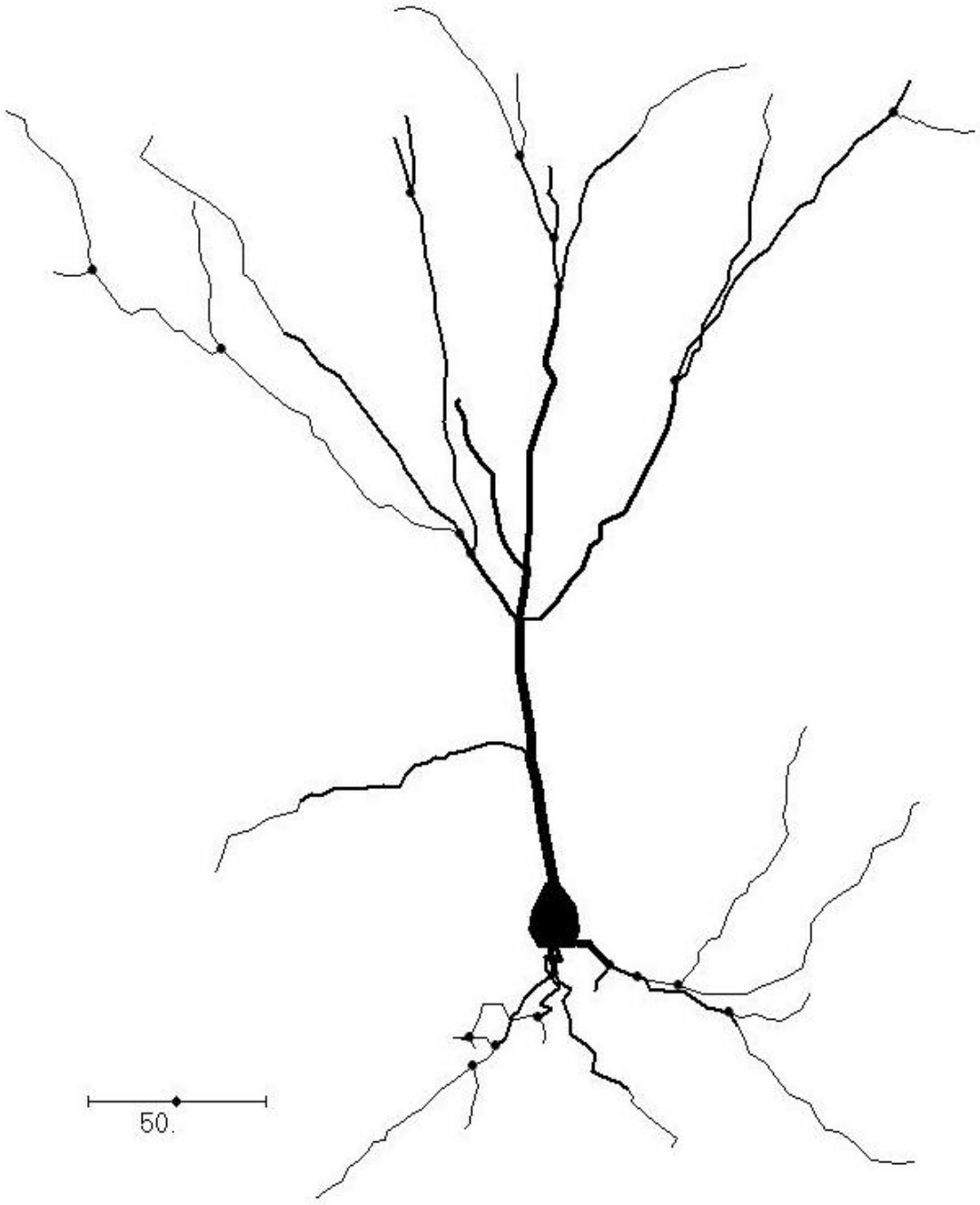

Figure 17. Group 2 representative neuron. Layer II pyramidal neurons (n=7 neurons) characterized by a nonbifurcating apical dendrite until after an average of 25.7 µm. The apical dendrites for Group 2 neurons are on average 17.4% (3.8 µm) longer than those of Group 1. Cells are oriented so that the pia is at the top of the page. Scale bar: 50 µm.

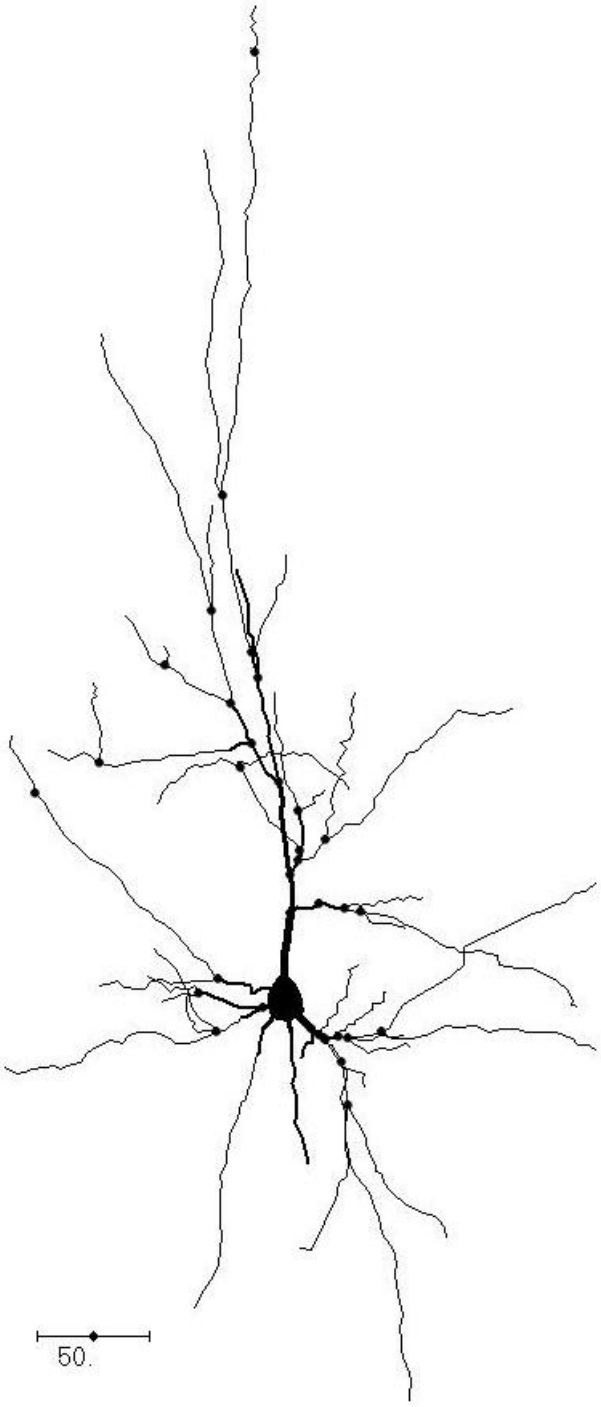

Figure 18. Group 3 representative neuron. These layer III (n=32 neurons) pyramidal neurons projected their apical dendrites through layers II and I sometimes reaching the pial surface. Cells are oriented so that the pia is at the top of the page. Scale bar: 50 µm.

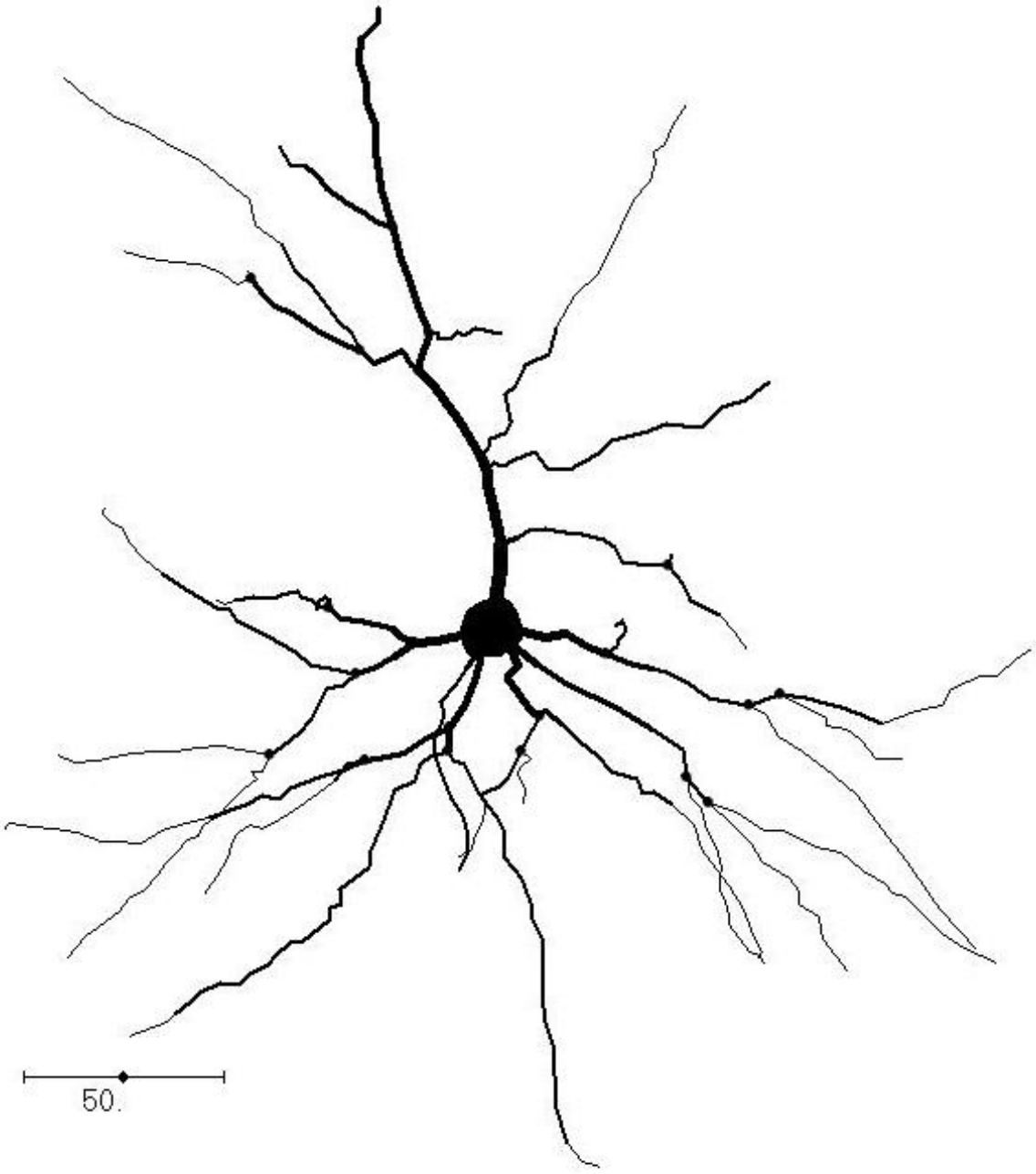

Figure 19. Group 4 representative pyramidal neurons of layers V and VI. These were the largest of the pyramidal neurons and exhibited the largest apical dendrite spread. Cells are oriented so that the pia is at the top of the page. Scale bar: 50 µm.

Group 5: Layer II-III nonpyramidal neurons

The neurons of Group 5 (n=12; 13.3% of total neuronal population) did not have a pyramidal shape nor did they exhibit a distinctive apical dendrite. Instead neurons in this group demonstrated dendrites projecting within the same layer in which their somas were found, as illustrated in Figure 25. Somatic characteristics for this group of neurons proved that they had the smallest overall soma from all groups identified. These included values for somatic perimeter (avg=51.8 µm; stdev=14.5 µm), somatic area (avg=160.0 µm²; stdev=38.7 µm²), feret max (avg=17.0 µm; stdev=2.9 µm), feret min (avg=12.5 µm; stdev=1.9 µm) and somatic aspect ratio (avg=1.4; stdev=0.2).

The dendritic characteristics of this group of neurons include the total number of dendrites (avg=3.8; stdev=1.6), a high number of total basilar nodes (avg=11.8; stdev=7.5) and a much greater total dendritic length (avg=1109.3 µm; stdev=721.9 µm) than the four groups of pyramidal neurons had. Other dendritic measurements were observed such as the mean length of individual dendrites (avg=303.2 µm; stdev=180.7 µm), the large dendritic surface area (avg=3281.0 µm²; stdev=2341.6 µm²), the mean dendritic surface area (avg=918.0 µm²; stdev=686.3 µm²), the total dendritic volume (avg=1027.3 µm³; stdev=862.7 µm³) and the mean dendritic volume (avg=293.2 µm³; stdev=277.0 µm³).

Group 5 nonpyramidal neurons had smaller overall total maximum horizontal spread (avg=172.4 µm; stdev=51.6 µm) than pyramidal neurons. This value was calculated by summing the horizontal spread of the medial aspect of the dendrites (avg=81.8 µm; stdev=46.7 µm) and the horizontal spread of the lateral aspect of the basilar dendrites (avg=90.6 µm; stdev=36.9 µm). This is indicative of the fact that Group 5 neurons have short, local dendritic processes. These results are grouped in Table A5.

Group 6: Layer V-VI nonpyramidal neurons

Just like the Group 5 neurons, Group 6 neurons (Figure 26) did not have clear pyramidal shapes with distinguishable apical dendrites pointing toward the pial surface. These neurons (n=15; 16.7% of total neuronal population) were oriented parallel to the pia and were found in close proximity to the grey-white border. They exhibited large somatic characteristics, including a somatic perimeter (avg=55.7 µm; stdev=8.7 µm), somatic area (avg=202.3 µm²; stdev=58.2 µm²), feret max (avg=19.7 µm; stdev=3.5 µm), feret min (avg=13.5 µm; stdev=2.0) and aspect ratio (avg=1.5; stdev=0.3).

Group 6 neurons exhibited the largest dendritic characteristics out of all six groups. They had a large number of dendrites (avg=3.9; stdev=1.6), the largest number of dendritic nodes (avg=13.9; stdev=6.3), the largest dendritic length (avg=1345.4 µm; stdev=630.0 µm) and mean individual dendritic length (avg=373.6 µm; stdev=208.4 µm). Also, these neurons exhibited the largest dendritic surface area (avg=5038.6 µm²; stdev=2944.9 µm²), mean individual dendritic surface area (avg=1420.9 µm²; stdev=1151.0 µm²), total dendritic volume (avg=2099.0 µm³; stdev=1710.7 µm³) and mean individual dendritic volume (avg=619.2 µm³; stdev=775.6 µm³) out of all six neuron groups.

When compared with Group 5 neurons, a major distinguishing characteristic of Group 6 neurons is the larger total maximum horizontal dendritic spread (avg=247.2 µm; stdev=153.4 µm) . This value was calculated by summing the horizontal spread of the medial aspect of the dendrites (avg=108.2 µm; stdev=48.7.7 µm) and the horizontal

spread of the lateral aspect of the basilar dendrites (avg=139.0 µm; stdev=47.1 µm). The morphological characteristics of Group 6 neurons are summarized in Table A6.

TABLE 7. Dendritic characteristics: nonpyramidal Groups 5-6

		DENDRITES							
Neuron Group		**Qty**	**Nodes**	**Length(µm)**	**mean len**	**Surface(µm²)**	**mean sur**	**Volume(µm³)**	**mean vol**
Layer II-III nonpyramidal neurons	avg	3.8	11.8	1109.3	303.2	3281.0	918.0	1027.3	293.2
	st dev	1.6	7.5	721.9	180.7	2341.6	686.3	862.7	277.0
Layer V-VI nonpyramidal neurons	avg	3.9	13.9	1345.4	373.6	5038.6	1420.9	2099.0	619.2
	stev	1.6	6.3	630.0	208.4	2944.9	1151.0	1710.7	775.6

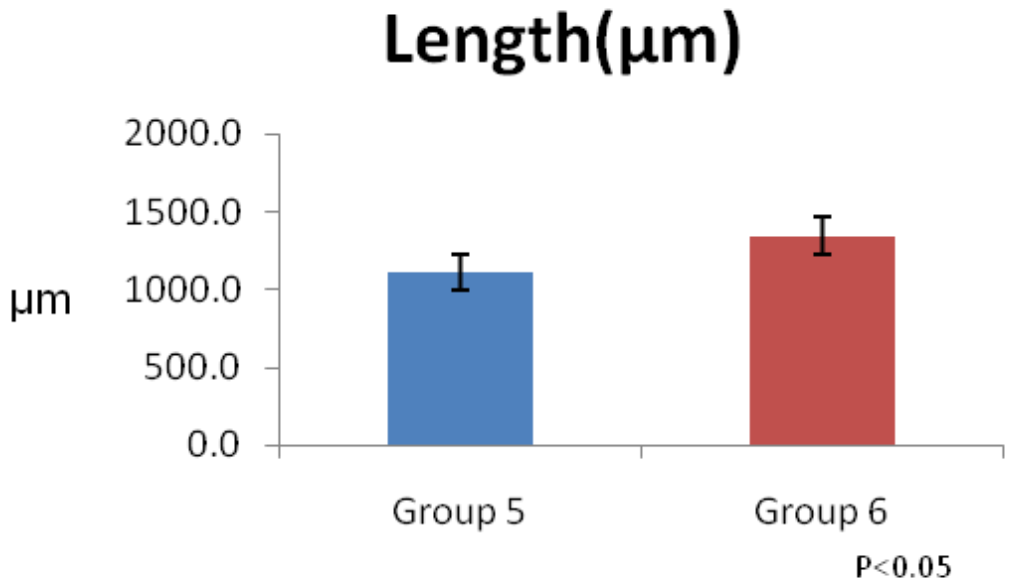

Figure 20. Dendritic length: Groups 5-6.

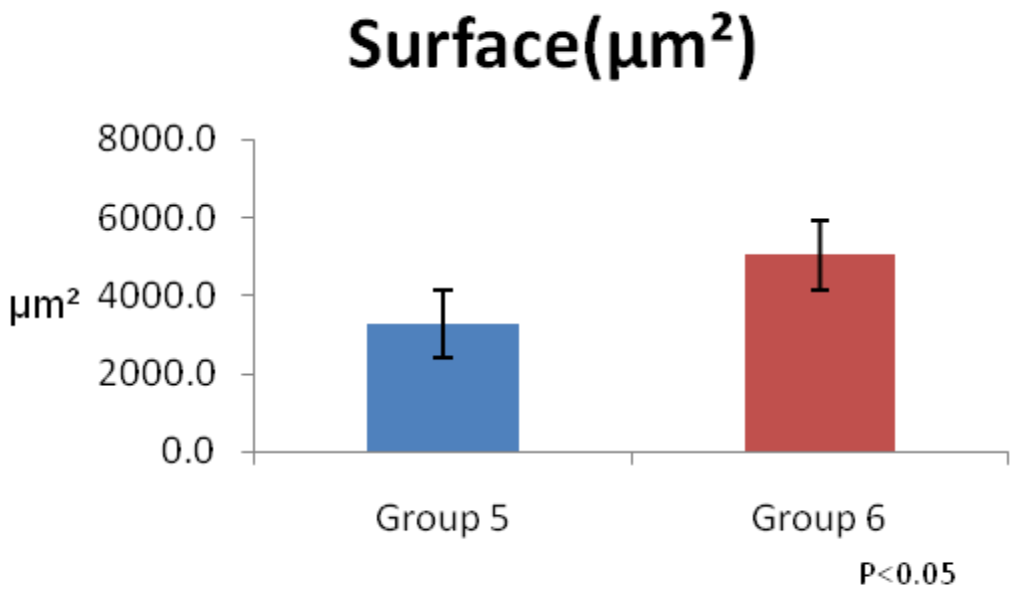

Figure 21. Dendritic surface area: Groups 5-6.

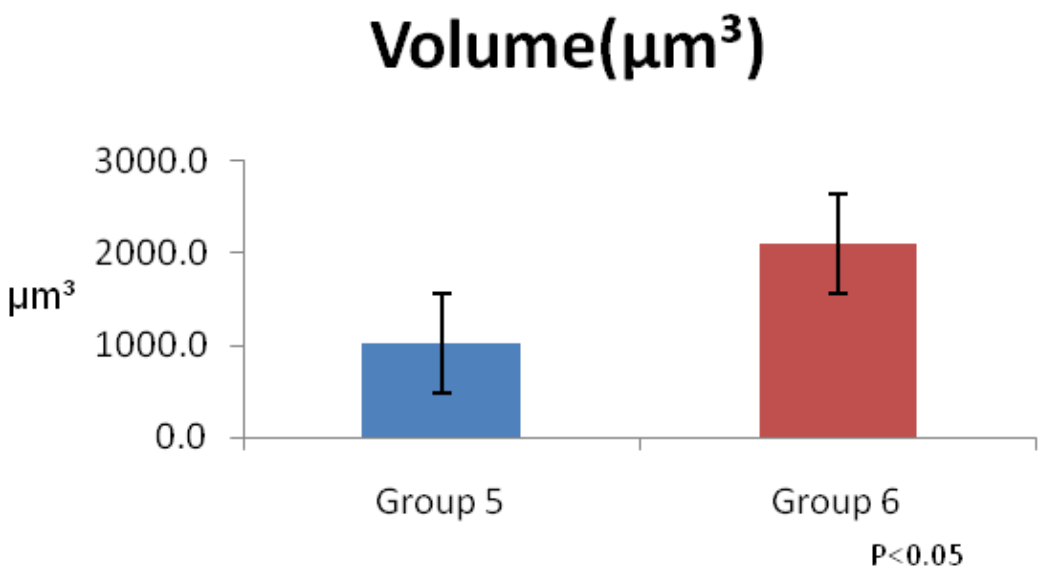

Figure 22. Dendritic volume: Groups 5-6.

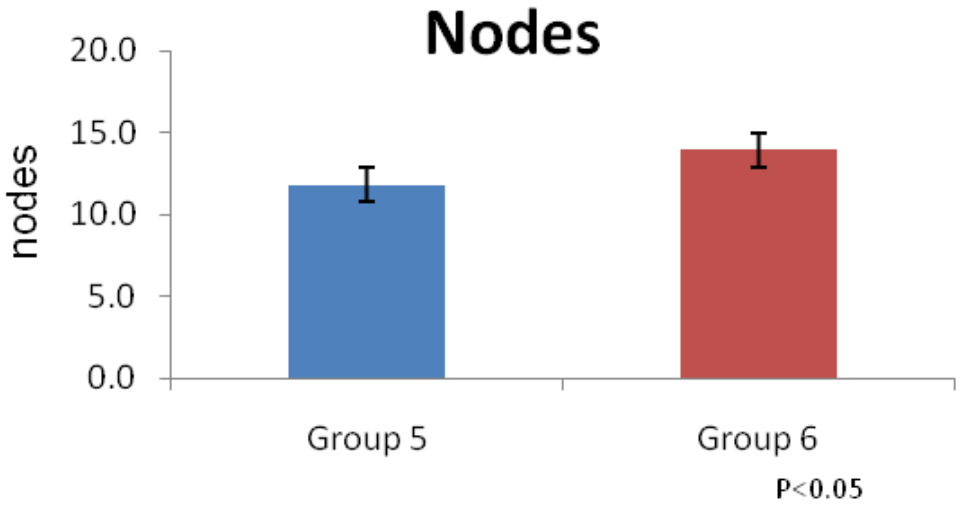

Figure 23. Dendritic nodes: Groups 5-6.

TABLE 8. Maximum horizontal spread: nonpyramidal Groups 5-6

Neuron Group		Maximum horizontal spread (µm)of nonpyramidal groups		
		medial	lateral	total
Layer II-III nonpyramidal	avg	81.8	90.6	172.4
	stdev	46.7	36.9	51.6
Layer V-VI nonpyramidal	avg	108.2	139.0	247.2
	stdev	48.7	47.1	153.4

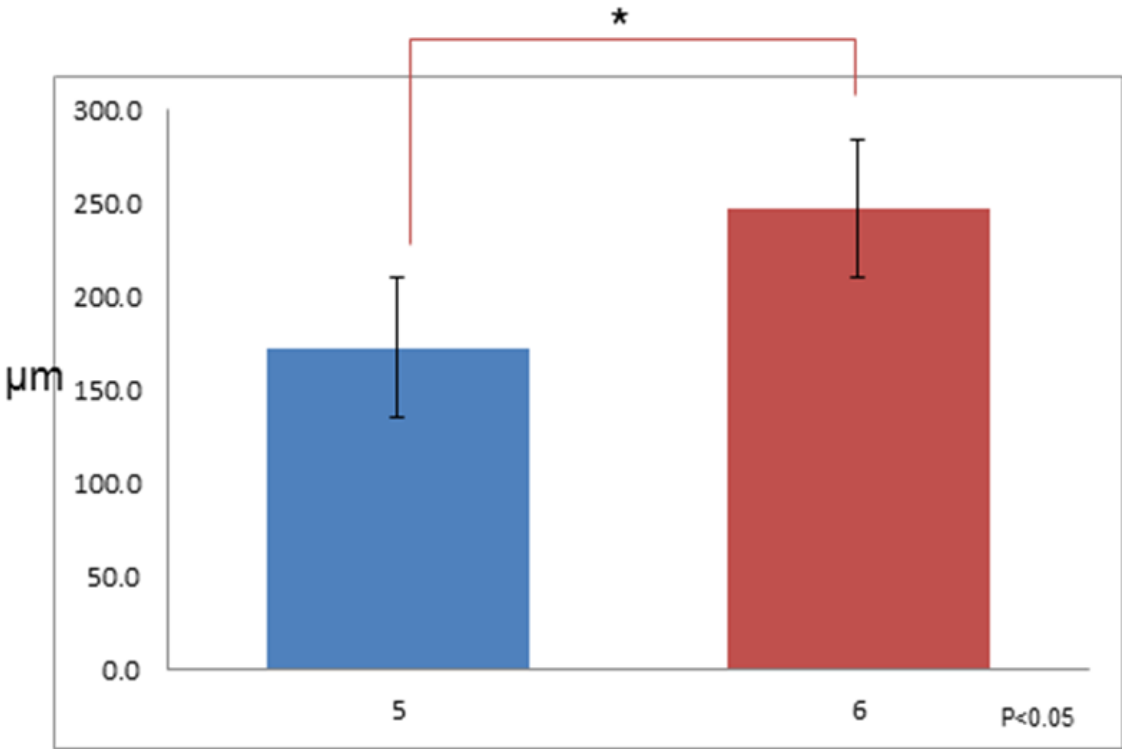

Figure 24. Maximum dendritic horizontal spread: Groups 5-6.

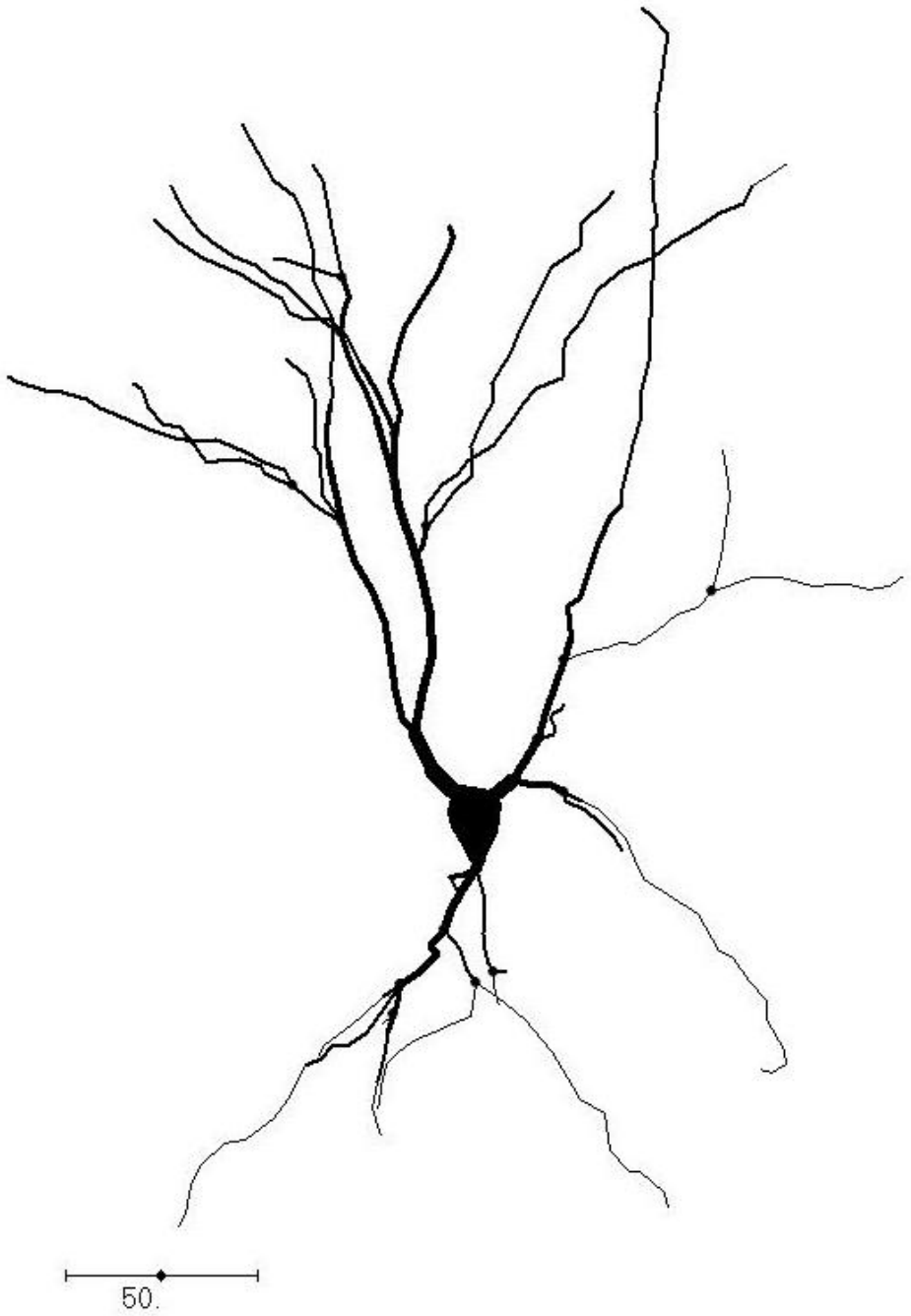

Figure 25. Group 5 representative neurons. These layer II and III nonpyramidal neurons had the smallest somatic area and horizontal dendritic spread of the two groups of nonpyramidal neurons. Cells are oriented so that the pia is at the top of the page. Scale bar: 50 µm.

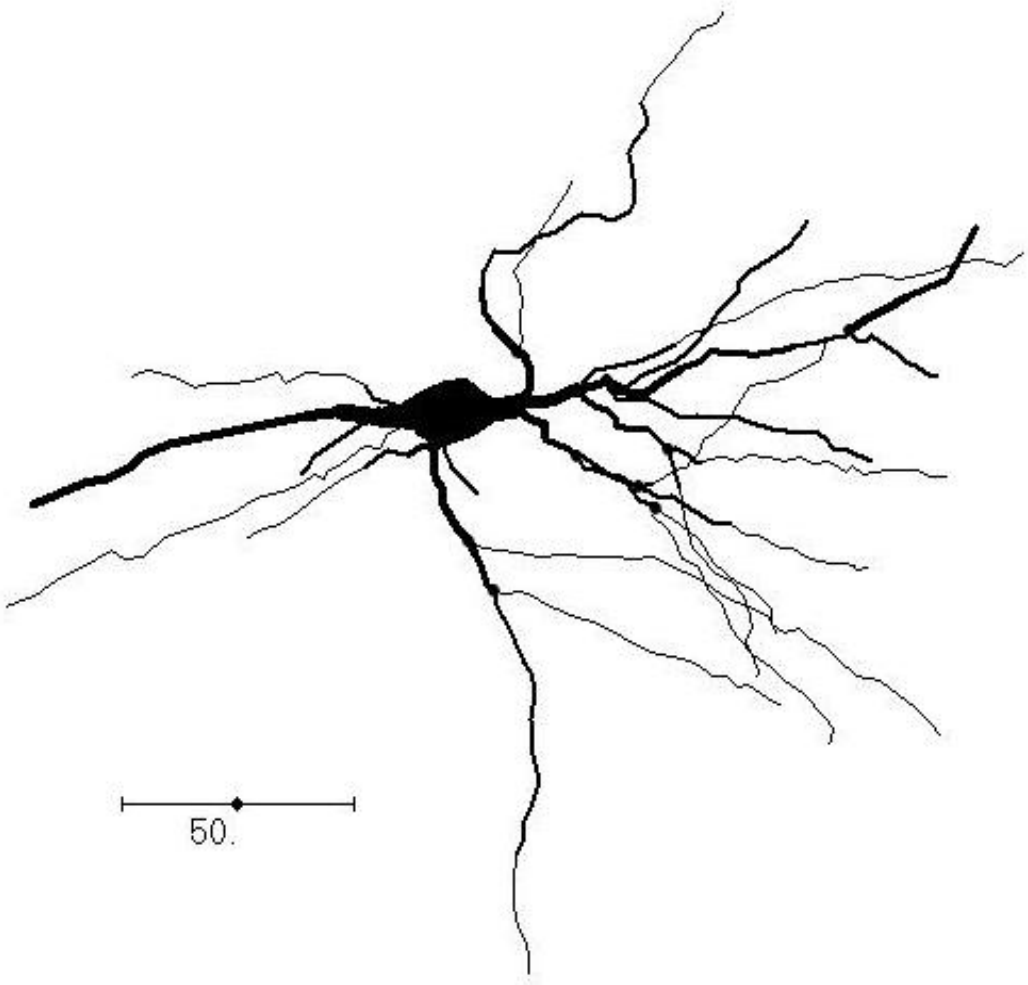

Figure 26. Group 6 nonpyramidal neurons of layers II and III. These neurons were found in close proximity to the grey-white border and were oriented parallel to the pial surface. Cells are oriented so that the pia is at the top of the page. Scale bar: 50 µm.

DISCUSSION

The results of this study address three interrelated themes. First, the basic cytoarchitectonic features of a multisensory (LRSS) cortical region and its distinctions from well-studied unimodal sensory areas are explored. Second, the morphological characteristics of the constituent neurons of the multisensory LRSS are compared with those of unimodal sensory cortical regions. Third, the character of a cortical column within the multisensory LRSS is being discussed and compared with that proposed for cortical primary sensory regions.

1. The Cytoarchitecture of the LRSS

The neocortex is characterized by the arrangement of its gray matter into six layers (Mountcastle, 1998), and the LRSS is consistent with this universal feature. The present study shows that the LRSS exhibits, from top to bottom, a typical layer I that is largely devoid of neuronal cell bodies. Its other, supragranular layers (layers II and III) are the thickest components of the region and contribute to over half of the area's volume. Using SMI-32 staining, layer II is distinguishable from layer III by its staining of vertically-ordered dendrites but lack of neuronal somata. By contrast, layer III is composed of heavily stained, medium-sized pyramidal neurons with vertical as well as oblique dendritic components labeled. Layer IV (also termed the 'granular' layer') was narrow and virtually unstained. Spiny stellate neurons that predominate in this layer in other cortical areas were not apparent in the LRSS. Layer V, like layer III, featured well-stained medium- and large-sized pyramidal neurons and their dendritic processes. In

contrast, layer VI revealed few stained neuronal somata and only occasional short dendritic processes. In summary, due to its narrow layer IV and apparent lack of stellate neurons, in addition to its distinct six-layered appearance and its relative location between unimodal sensory cortical areas, the LRSS can be categorized as being a "granular homotypical neocortex".

The LRSS divides the primary somatosensory cortex (SI) medially (Rice et al., 1993) from a region of four (AVF, ADF, AAF and A1) auditory fields (Bizley et. al, 2005; Kowalski et al., 1995) laterally. The LRSS is bordered caudally by the visual anteriolateral lateral suprasylvian (ALLS) area (Homman-Ludiye et al, 2010). Given its location between representations of three different sensory modalities (see Figure 1), it is not surprising that functional studies of the LRSS have observed amongst the highest levels of multisensory neurons (~62%) reported for cortex (Keniston et al., 2008). Therefore, one issue addressed by the present study is to describe the cytoarchitectural features of the multisensory LRSS and to compare that with descriptions of unisensory cortical representations.

Keniston (2009) used SMI-32 antibody labeling to examine the cytoarchitecture of the medial bank of the rostral suprasylvian sulcal (MRSS) region, a higher-level somatosensory area adjacent to the SI in the ferret. This study found the MRSS to have expanded and densely populated cortical layers II and III containing small pyramidal cells and granule cells. In addition, Layer IV in the MRSS was described as being very narrow and sparsely populated, while layers V and VI comprised of small pyramidal cells. An earlier study (Bajo et al, 2007) using Nissl and SMI-32 staining described the cytoarchitecture of the ectosylvian gyrus of the ferret, a region which contains the

auditory areas AVF, ADF, AAF and A1. The AVF and ADF regions showed a granular pattern in layers II and III in addition to containing very large pyramidal neurons in layer V. The AAF and A1 regions showed an even stronger granular pattern than the AVF and ADF regions, revealing a bilaminar pattern of staining. More evidence of large layer V pyramidal neurons in the AVF region was later described (Bajo et al, 2010) as well. Also described was a change in laminar structure for the area anterior to the AVF, currently believed to be the second somatosensory area (SII), with more intense staining found in layer II and III outside the auditory cortex (Bizley, 2005). A recent study (Homman-Ludiye et al., 2010) has provided evidence for the homology between the ferret visual cortex and the well-studied cat extrastriate visual cortex (Palmer, 1978; Tusa, 1979; Albus, 1980; Tusa, 1980, Van der Gucht, 2001) and discussed the ferret ALLS which is located caudal to the LRSS. This area contained large layer V neurons possessing a thick apical dendrite which terminates in layer III. It was also described to have smaller layer III pyramidal neurons with large basilar dendritic arborization and an apical dendrite extending into layer II in addition to a small number of layer IV stellate-like neurons. Except for the layer IV stellate neurons, these neuronal features were also observed in the present study of the LRSS.

In parallel to these granular cytoarchitectonic features of higher-level sensory cortices, primary sensory areas are characterized by a wide and even, sub-laminated layer IV, which has also been described as a "granular" cortex. Layer IV of cat primary auditory cortex shows two sublaminae (Winer, 1984). Layer IV of the primate visual cortex exhibits four sublaminae (Lund et al., 2003), which are densely populated with spiny stellate and small pyramidal neurons. Spiny stellate neurons, which are the

principal thalamorecipient neurons of the region, have also been identified in S1 barrel cortex of rodents (Schubert et al., 2007; Woolsey and Van der Loos, 1970; Welker, 1974; Fox, 2002; Glazewski, 1996) and cat primary auditory cortex (Winer, 1984). In fact, Winer (1984) described a population of six distinct types of small non-pyramidal neurons with characteristic neuronal architecture and intracortical axonal branches in layer IV of A1 cortex. However, a lack of layer IV SMI-32 staining similar to the one in the present study was also reported by recent work in the cat AI and AAF (Mellott et al, 2010), in addition to a study on the entorhinal cortex of the fruit bat (Gatome et al, 2010) describing a distinct but cell-sparse layer IV. Ramsay and Meredith (2003) also reported a narrow laminae IV in the ferret multisensory PSSC region using biotinylated dextran amine (BDA) tracer. One possibility for future studies involving layer IV is to employ the recently discovered molecular markers RORB and EAG2 (Rowell et al, 2010) in order to visualize the neuronal population of this layer. Ultimately, however, the present study indicates that major cytoarchitectonic features distinguish the multisensory LRSS region from primary sensory cortices.

2. Neuronal Morphology

These results show that the neurons of the ferret multisensory LRSS region are varied in their morphological properties but can be grouped into 6 distinct populations based on shared morphological characteristics. The reconstructed neurons presented in the current study fell into two major categories: pyramidal (displaying an apical dendrite emerging vertically towards the pia) and nonpyramidal (neurons without such an apical dendrite). Furthermore, each of the two main categories can be further divided into a total

of six distinct neuronal populations based largely, but not exclusively, on their laminar location (groups 1, 2, 3 and 4 being pyramidal neurons; groups 5 and 6 were nonpyramidal neurons).

Group 1 neurons are layer II pyramidal neurons which have a clear and symmetrical bifurcation in their apical dendrite. These neurons exhibit the largest apical dendrite length, apical dendrite surface area, apical dendrite volume and number of apical dendrite nodes out of the four groups of pyramidal neurons. Their first apical bifurcation was located at an average distance from the soma of less than 22 µm and had the second largest total apical horizontal spread. They also represent the pyramidal neuronal population with the smallest basilar dendrite surface area and basilar dendrite volume.

Group 2 neurons are layer II pyramidal neurons that exhibited a single apical dendrite that often extended to the pial surface and whose initial apical branch was at an average of 25.7 µm away from the soma. These neurons had the smallest somatic surface area out of the pyramidal groups; however they had the largest maximum total basilar dendrite horizontal spread and largest basilar dendrite surface area. This spread could be an indication that Group 2 neurons receive a large number of inputs from the surrounding neuronal population.

Neurons of Group 3 were the most populous group. These cells were located in the third cortical layer and sent their apical dendrites into layer II. Out of the four groups of pyramidal neurons, they ranked third in terms of the somatic area, however they exhibited the largest distance from the soma to the first apical branch point. They had the smallest apical dendrite length, smallest number of apical dendrite nodes and smallest total apical maximum horizontal spread.

Group 4 pyramidal cells of layer V and VI are the largest of the pyramidal cells in terms of the somatic area. Their initial apical branch was very close to the soma (~10 µm compared with the second smallest group, Group 1, which was ~ 22 µm); however they exhibit the largest apical dendrite total horizontal spread and the second largest number of apical dendrite nodes out of the pyramidal neurons. Although they had the second highest number of basilar dendrites out of the pyramidal cells, they had the smallest basilar dendrite nodes, basilar dendrite length and second smallest basilar dendrite surface area and volume.

Of the two groups of nonpyramidal neurons, Group 5 contained the smallest cells. These layer II-III neurons had the smallest somatic area and the smallest total dendritic horizontal spread out of all six groups of neurons as well.

Group 6 nonpyramidal neurons of Layers V-VI had larger somatic areas, total dendritic horizontal spread, number of branches, number of bifurcations, dendritic length, dendritic surface area and dendritic volume than their layer II-III counterparts.

There is a large literature, dating back to the studies of Cajal (1899), describing the distinctive morphological features of neurons from various areas of the brain using the Golgi-impregnation technique. The results of the current study are consistent with these previous data by showing marked differences and variability in morphology between pyramidal neurons of the supragranular and infragranular cortical layers (see also Porter et al., 1991). Furthermore, similar observations were made in an examination of the multisensory area STS in the macaque monkey (Elston, 2001). Therefore, it seems likely that the present technique adequately and appropriately demonstrated the morphological features that were examined.

Other morphological studies of cortical neurons have described even more extensive distinctions and groups than identified here. For example, Layer II alone (Winer, 1985b) was described as having eight varieties of neurons belonging to both the pyramidal and non-pyramidal classes. In fact, in the exhaustive study of cat primary auditory cortex, Winer and colleagues identified 8 types of neurons in layer II (Winer, 1985b), 12 types in layer III (Code & Winer, 1985), 6 types in layer IV (Winer, 1985), 7 types in layer V(Winer & Prieto, 2001) and 9 types in layer VI (Prieto & Winer, 1999). Similarly, other studies identified multiple forms of glutamatergic neurons in layer VI (Andjelic et al., 2009; Briggs, 2010). Therefore, it seems likely that the number of neuron groups identified in the present study is an underestimation of the variability that could be present. Several factors inherent to this study may account for this. One of these is the thin sectioning of the Golgi-impregnated tissue. The serial slices were only 100 µm thick in this study compared to slices of up to 300 µm in Winer (1985), possibly leading to neuronal branch cutoff (the widest neuronal dendritic spread was 250.9 µm) and providing for only a partial representation of dendritic arbors; therefore the possibility for cutoff of up to 150.9 µm (250.9 µm wide arbor minus 100 µm thick section = 150.9 µm difference) is a realistic inherent problem. However, previous studies have used sections of varying thickness such as 60 µm (Prieto and Winer, 1999), 50-100 µm (Winer and Prieto, 2001), 250 µm (Elston, 2001), 200-250µm (Chen et al, 2009), therefore no one section thickness can be said to be more indicative than the others. Another factor can be the incomplete Golgi-Cox stain infiltration due to the nature of the staining method itself. It is approximated that only 10% of neurons get stained via the Golgi-Cox, with no mechanism to explain this phenomenon being described so far, therefore every study

using this technique is bound to have a methodological limitation. Finally, the total number of neurons reconstructed (90) might provide an incomplete representation of the total neuronal population; however, previous studies have analyzed quantities both larger (222 neurons in Chen et al., 2009; 139 neurons in Elston, 2001) and smaller (~70 neurons in Winer and Prieto, 2001) that the one in the present study.

While analyzing the dendritic properties of pyramidal neurons, Winer (1985) described their lateral basilar dendritic fields to approximate 350 µm and somatic areas of 225 µm². The present study described Groups 1 and 2 neurons as being pyramidal and having lateral basilar spread of 202 µm and 251 µm and somatic areas of 203 µm² and 183 µm² respectively. Layer III was previously studied in the cat AI (Code and Winer, 1985) with a description of 12 different kinds of neurons that contribute to the commissural system. Of those, the pyramidal cells had somatic areas of 294.8 µm² and the non-pyramidal cells had somatic areas of 216.9µm². The present study describes Group 3 pyramidal neurons of the LRSS layer III as having a somatic size of 200.8 µm² and Group 5 nonpyramidal neurons of layers II and III having a somatic area of 160.0 µm². Winer and Prieto also studied layer V in the cat AI (Winer and Prieto, 2001) and found a total of seven different types of neurons (4 pyramidal and 3 nonpyramidal) with significant differences in somatic size between them. Their study found pyramidal neurons to have a somatic area between 272 µm² and 1200 µm² and between 3 and 6 primary dendrites per neuron. The present study showed Group 4 neurons (layer V-VI pyramidal) to have a somatic area of 206.9 µm² and to average 3.8 basilar dendrites per neuron. And the size of the layer V pyramidal neuron was described in the cat AAF and

AI by Mellott (2010) as well. The mean somatic area for the AAF was 381 μm² and for the AI was 433 μm².

3. The LRSS Cortical Column

It is well established that the cortical laminar patterns contribute to cortical connectivity. Specifically, supragranular layer II-III neurons exhibit efferent projections that target other cortical areas, while layer V-VI neurons connect with subcortical and brainstem regions. The present study did not examine these extrinsic connectional features. On the other hand, there is compelling evidence for intrinsic cortical processing in the vertical dimension, which the present results can address. The vertical, trans-laminar arrangement of intracortical connections is largely regarded currently as a cortical column. The idea of the cortical column was first proposed by Mountcastle (Mountcastle, 1957) after noticing a vertical organization of neurons and their closely related functional properties and reading Lorente de No's Golgi studies (Lorente de No, 1938) describing a predominance of vertical connections between neurons in the cortex. The present investigation of LRSS neurons revealed, especially for the pyramidal neurons, a strong vertical orientation of apical dendrites that spanned several laminae and were consistent with descriptions of pyramidal neurons elsewhere in the neocortex (Chen et al., 2009, Elston, 2001; Mountcastle, 1998; Feldman, 1984). As depicted in Figure 27 when neurons of the different groups were reconstructed and graphically stacked, their arrangement recreates the vertical organization of neurons in the LRSS. Although local connectivity could not be studied in these anatomical treatments, the arrangement illustrates a presumptive column within the LRSS cortex.

Although a great deal of functional data supports the notion of cortical columnar organization (Panzeri, 2003; Foffani, 2008; Meyer, 2010a; Meyer 2010b; Wimmer, 2010), an anatomical demonstration of the concept is lacking. Nevertheless, from anatomical data, it is possible to estimate the width of a generic cortical column by determining the width of the participating dendritic trees. Accordingly, a cortical column in monkey primary visual cortex has been measured to be ~250-300 um in width (Lund, 2003). From the present study, stacking neurons in their appropriate layers in vertical alignment (Figure 27) suggests a column in LRSS would be at least as wide as the widest dendritic arbors of 250.9 µm. This figure may be an underestimation because the entire dendritic tree was not reconstructed from these 100 um thick sections and, thus, the possibility of not observing the widest branches or terminal ends of the neurons sampled. Despite these caveats, the data summarized in Figure 27 provides a first approximation of features for this important processing unit in multisensory cortex

Lately, the notion of a column has been modified to include the concept of a hypercolumn and the minicolumn (Buxhoeveden and Casanova, 2002; Mountcastle, 2003). The hypercolumn is a set of neighboring cortical columns exhibiting an orderly progression of their parameters and requiring approximately 1 mm of cortical space (Hubel and Wiesel, 1977). These authors speculated through the "ice cube model" that an orthogonal arrangement between two such hypercolumns would provide a region of optimal interaction between two sets of cortical properties, perhaps forming a 1 mm^2 area of sensory integration. In contrast, the 40-50 µm wide minicolumn contains neurons with a single set of similar properties and is regarded as the basic unit of cortical operation (see Canonical microcircuit, below). The present data from the LRSS does not

address either of these modifications of the cortical column, as both are based on functional, not anatomical, measures.

To many investigators, the presence of relatively few types of excitatory and inhibitory neurons linked together into a vertical unit is suggestive of a canonical microcircuit that is repeated across a cortical area and across the entire cortex (Douglas, 1989). Furthermore, It is established that supragranular layer pyramidal neurons receive feedforward excitatory input from subcortical (thalamic), inter-areal and intra-areal sources (Douglas and Martin, 2004). These neurons also receive recurrent input from neighboring supragranular pyramidal cells and also from infragranular pyramidal cells and provide outputs mediated by horizontal smooth cells which control the activation patterns of vertical smooth cells. Infragranular layer V pyramidal neurons provide feedback projections to the supragranular layers of other cortical areas in addition to providing outputs to the basal ganglia, colliculus and ventral spinal cord. They also form connections with layer VI pyramidal neurons, which, in turn, form connections with the thalamic input layers. Thus, it is likely with further investigation, that the features of LRSS neurons revealed here will ultimately be integrated within a broader system of connectivity and function. Whether these features of a multisensory cortex are similar to, or different from, those described for unisensory primary cortices remains to be determined.

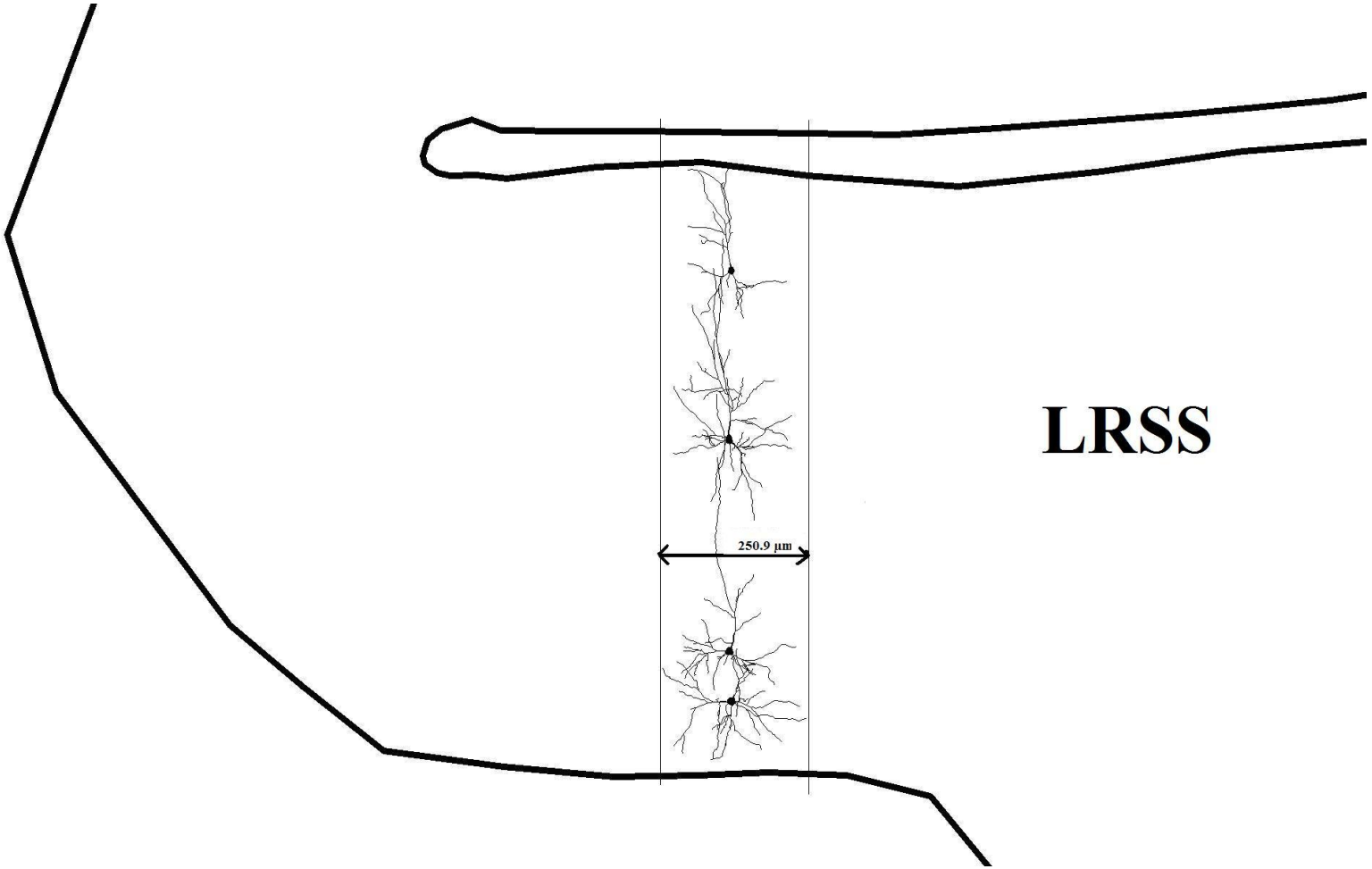

Figure 27. Presumptive columnar organization of LRSS neurons. Neurons from the different groups are stacked vertically according to their laminar location and distribution. The maximum width of the dendritic arbors contained within this column averaged 250.9 µm wide.

List of References

Albus, K., Beckmann, R. (1980). Second and third visual areas of the cat: interindividual variability in retinotopic arrangement and cortical location. J Phisiol 299:247-276.

Allman, B.L., Bittencourt-Navarrete, R.E., Keniston, L.P., Medina, A., Wang, M.Y., Meredith, M.A. (2008). Do cross-modal projections always result in multisensory integration? Cereb Cortex 18:2066–2076

Andjelic S., Gallopin T., Cauli B., Hill E.L., Roux L., Badr S., Hu E., Tamas G., Lambolez B. (2009). Glutamatergic nonpyramidal neurons from neocortical layer VI and their comparison with pyramidal and spiny stellate neurons. J Neurophysiol 101:641-654.

Bajo, V.M., Nodal, F.R., Bizley, J.K., Moore, D.R., King, A.J. (2007). The ferret auditory cortex: descending projections to the inferior colliculus. Cereb Cortex 17:475-491.

Bajo, V.M., Nodal, F.R., Moore, D.R., King A.J. (2010). The descending corticocollicular pathway mediates learning-induced auditory plasticity. Nature Neuroscience 13:253–260

Benevento L.A., Fallon J., Davis B.J., and Rezak M. (1977). Auditory-visual interaction in single cells in the cortex of the superior temporal sulcus and the orbital frontal cortex of the macaque monkey. Exp Neurol 57: 849-872

Bizley J.K., Nodal F.R., Bajo V.M., Nelken I., King A.J. (2007). Physiological and anatomical evidence for multisensory interactions in auditory cortex. Cereb Cortex 17:2172-2189

Bizley J.K., Nodal F.R., Nelken I., King A.J. (2005). Functional organization of ferret auditory cortex. Cereb Cortex 2005. 15:1637-1653.

Bizley, J. K., and King, A. J. (2008). Visual-auditory spatial processing in auditory cortical neurons. Brain Res. 1242:24–36

Bizley, J. K., and King, A. J. (2009). Visual influences on ferret auditory cortex. Hear. Res. 258, 55–63.

Briggs, F. (2010). Organizing principles of cortical layer 6. Front Neur Circuits 4:1-8.

Bruce C., Desimone R., and Gross C.G. (1981). Visual properties of neurons in a polysensory area in superior temporal sulcus of the macaque. J Neurophysiol 46: 369-384.

Buxhoeven, D.P., Casanova, M. (2002). The minicolumn hypothesis in neuroscience. Brain. 125:935-951

Callaway, E.M. and Katz, L.C. (1993). Photostimulation Using Caged Glutamate Reveals Functional Circuitry in Living Brain Slices. Proceedings of the National Academy of Sciences of the United States of America. 90:7661-7665.

Calvert, G. A., Campbell, R. & Brammer, M. J. (2000). Evidence from functional magnetic resonance imaging of crossmodal binding in the human heteromodal cortex. Curr. Biol. 10:649–657.

Chen, C.C., Abrams, S., Pinhas, A., Brumberg, J.C. (2009). Morphological heterogeneity of layer VI neurons in mouse barrel cortex. J Comp Neurol 512:726-746.

Code, A.R., Winer J.A. (1985). Commisural neurons in Layer III of cat primary auditory cortex (AI): Pyramidal and Non-pyramidal cell input. J Comp Neurol 242:485-510.

Douglas, R.J., Martin K.A.C. (2004). Neuronal circuits of the neocortex, Annual Reviews in Neuroscience 27:419–451.

Douglas, R.J., Martin, K.A.C., Witteridge, D. (1989). A canonical microcircuit for neocortex, Neural Computation 1:480–488.

Elston, G. N. (2001). Interlaminar differences in the pyramidal cell phenotype in cortical areas 7m and STP (the superior temporal polysensory area) of the macaque monkey. Exp Brain Res 138:141-152

Faherty, C.J., Kerley, D., Smeyene, S.J. (2003). A Golgi-Cox morphological analysis of neuronal changes induced by environmental enrichment. Dev Brain Res 141:55-61.

Feldman, M.L. (1984). Morphology of the neocortical pyramidal neuron. In: Peters A, Jones EG (eds) Cerebral Cortex, vol 1: Cellular Components of the cerebral cortex. Plenum, New York. pp 123-200.

Foffani, G., Chapin, J.K., Moxon, K.A. (2008). Computational role of large receptive fields in the primary somatosensory cortex. J Neurophysiol 100:268–280.

Fox, K. (2002) Anatomical pathways and molecular mechanisms for plasticity in the barrel cortex. Neuroscience 111:799–814

Furtak, S.C., Moyer, J.R., Brown, T.H. (2007). Morphology and ontogeny of rat perirhinal cortical neurons. J Comp Neurol 505:493-510.

Gatome C.W., Slomianka L., Mwangi D.K., Lipp H.P, Amrein I. (2010). The entorhinal cortex of the Megachiroptera: a comparative study of Wahlberg's epauletted fruit bat and the straw-coloured fruit bat. Brain Struct. Funct. 214:375-393.

Ghazanfar A.A., Chandrasekaran C., Logothetis N.K. (2008). Interactions between the superior temporal sulcus and auditory cortex mediate dynamic face/voice integration in rhesus monkeys. J Neurosci 28:4457–4469.

Ghazanfar A.A., Maier J.X., Hoffman K.L., Logothetis N.K. (2005). Multisensory integration of dynamic faces and voices in rhesus monkey auditory cortex. J Neurosci 25:5004–5012.

Glazewski, S., Fox, K. (1996). Time course of experience-dependent synaptic potentiation and depression in barrel cortex of adolescent rats. J Neurophysiol 75:1714-1729

Homman-Ludiye, J., Manger, P.R., Bourne, J.A. (2010). Immunohistochemical parcellation of the ferret (Mustela putorius) visual cortex reveals substantial homology with the cat (Felis catus). J Comp Neurol 518:4439-4462.

Howard, I.P and Templeton, W.B. (1966). *Human Spatial Orientation.* London: Wiley.

Hubel, D.H., Wiesel, T. (1977). Functional architecture of macaque monkey cortex. Proc R Soc Lond B 198:1-59.

Jääskeläinen, I.P. (2010). The Role of Speech Production System in Audiovisual Speech Perception. Open Neuroimag J. 4:30–36.

Keniston, L.P, Allman, B.A., Meredith, M.A. (2008). The lateral rostral suprasylvian sulcus (LRSS) of the ferret: a 'new' multisensory area. Soc Neurosci Abstr 38:457.10.

Keniston, L.P., Allman, B.A., Meredith, M.A., Clemo, H.R. (2009). Somatosensory and multisensory properties of the medial bank of the ferret rostral suprasylvian sulcus. Exp Brain Res 196:239–251

Kowalski, N.,Vershnel, H., Shamma, S.A. (1995). Comparison of responses in the anterior and primary auditory fields of the ferret cortex. J Neurophysiol 73(4):1513-1523

Leinonen L., Hyvarinen J., and Sovijarvi A.R.. (1980) Functional properties of neurons in the temporo-parietal association area of the awake monkey. Exp Brain Res 39: 203-215.

Lorente de No, R. (1938) The cerebral cortex: architecture, intracortical connections, motor projections. In: Fulton J.F., editor. Physiology of the nervous system. London: Oxford University Press. pp 274-301.

Lund J.S., Angelucci, A., Bressloff, P.C., (2003). Anatomical substrates for functional columns in macaque monkey primary visual cortex. Cereb Cortex 13:15-24.

McGurk, H. and MacDonald, J. (1976). Hearing lips and seeing voices. Nature 264:229–239

Mellott, J.G., Van der Gucht, E., Lee, C.C., Carrascoa, A., Winer, J.A., Lomber, S.G. (2010). Areas of cat auditory cortex as defined by neurofilament proteins expressing SMI-32. Hear Res 267:119-136.

Meyer, H.S., Wimmer, V.C., Hemberger, M., Bruno, R.M., de Kock, C.P., Frick, A., Sakmann, B., Helmstaedter, M. (2010a). Cell type-specific thalamic innervation in a column of rat vibrissal cortex. Cereb Cortex 20:2287-2303.

Meyer, H.S., Wimmer, V.C., Oberlaender, M., de Kock, C.P., Sakmann, B., Helmstaedter, M. (2010b). Number and laminar distribution of neurons in a thalamocortical projection column of rat vibrissal cortex. Cereb Cortex. 20:2277-2286

Mountcastle, V.B. (1957). Modality and topographic properties of single neurons of cat's somatic sensory cortex. J Neurophysiol 20:408-434.

Mountcastle, VB. 1998. Perceptual Neuroscience: the cerebral cortex. Cambridge, MA: Harvard University Press.

Mountcastle, V.B. (2003). Introduction. Cereb Cortex 13:2-4

Palmer, L.A., Rosenquist, A.C, Tusa, R.J. (1978). Retinotopic organization of lateral suprasylvian visual areas in cat. J Comp Neurol 177:237-256.

Pandya, D.N., Seltzer, B. (1982). Intrinsic connections and architectonics of posterior parietal cortex in the rhesus monkey. J Comp Neurol 204:196–210.

Panzeri, S., Petroni, F., Petersen, R.S., Diamond M.E. (2003). Decoding Neuronal Population Activity in Rat Somatosensory Cortex: Role of Columnar Organization. Cereb. Cortex 13:45-52.

Porter, L.L., Ghosh, S., Lange, G.D., Smith T.G. (1991). A fractal analysis of pyramidal neurons in mammalian motor cortex. Neurosci Lett 130:112-116.

Prieto, J.J., Winer, J.A. (1999). Layer VI in cat primary auditory cortex: Golgi study and sublaminar origins of projection neurons. J Comp Neurol 404:332-358.

Ramón y Cajal, S. (1899). Comparative study of the sensory areas of the human cortex.

Ramon-Moliner, E. (1970). The Golgi-Cox technique. In: Nauta WJH, Ebbesson SOE, editors. Contemporary methods in neuroanatomy. New York:Springer.

Ramsay, A.M. and Meredith, M.A. (2003). Multiple sensory afferents to ferret pseudosylvian sulcal cortex. Neuroreport 15:461–465

Rice, F.L, Gomez, C.M., Leclerc, S.S., Dykes, R.W., Moon, J.S, Pourmoghadam, K. (1993). Cytoarchitecture of the ferret suprasylvian gyrus correlated with areas containing multiunit responses elicited by stimulation of the face. Somatosens Mot Res 10:161-188.

Rowell J.J., Mallik A.K., Dugas-Ford, J., Ragsdale, C.W. (2010). Molecular analysis of neocortical layer structure in the ferret. J Comp Neurol 518:3272–3289.

Sams M., Aulanko R., Hämäläinen M., Hari R., Lounasmaa O.V., Lu S.T., Simola J. (1991). Seeing speech: visual information from lip movements modifies activity in the human auditory cortex. Neurosci. Lett. 127:141–145.

Schroeder C.E., Foxe J.J. (2002). The timing and laminar profile of converging inputs to multisensory areas of the macaque neocortex. Cognitive Brain Research 14:187–198.

Schubert, D., Kötter, R. & Staiger, J.F. (2007) Mapping functional connectivity in barrel-related columns reveals layer- and cell type-specific microcircuits. Brain Struct. Funct., 212:107–119.

Smiley J.F., Hackett T.A., Ulbert I., Karmas G., Lakatos P., Javitt D.C., Schroeder C.E. (2007). Multisensory Convergence in Auditory Cortex: I. Cortical Connections of the Caudal Superior Temporal Plane in Macaque Monkeys. J Comp Neurol 502:894–923.

Stein, B.E and Meredith, M.A. (1993). *The Merging of the Senses.* Cambridge: MIT Press.

Tusa, R.J., Palmer L.A, Rosenquist, A.C. (1978) The retinotopic organization of area 17 (striate cortex) in the cat. J. Comp. Neurol. 177: 213–236.

Tusa R.J, Palmer L.A. (1980). Retinotopic organization of areas 20 and 21 in the cat. J Comp Neurol 193:147-164.

van der Gucht, E., Vandesande, F., Arckens, L. (2001). Neurofilament protein: a selective marker for the architectonic parcellation of the visual cortex in adult cat brain. J Comp Neurol 41:345-368.

Welker, C., Woolsey, T.A. (1974) Structure of layer IV in the somatosensory neocortex of the rat: description and comparison with the mouse. J Comp Neurol 158:437–454

Wimmer, V.C., Bruno, R.M., de Kock, C.P., Kuner, T., Sakmann, B. (2010). Dimensions of a projection column and architecture of VPM- and POm-axons in rat vibrissal cortex. Cereb Cortex. 20: 2265 -2276.

Winer, J.A. (1984). Anatomy of Layer IV in cat primary auditory cortex (AI). J Comp Neurol 224:535-567

Winer, J.A. (1985b). Structure of Layer II in cat primary auditory cortex (AI). J Comp Neurol 238:10-37.

Winer, J.A., Prieto, J.J. (2001). Layer V in cat primary auditory cortex (AI): Cellular architecture and identification of projection neurons. J Comp Neurol 434:379-412.

Woolsey, T.A. & Van der Loos, H. (1970) The structural organization of layer IV in the somatosensory region (SI) of mouse cerebral cortex. The description of a cortical field composed of discrete cytoarchitectonic units. Brain Res., 17:205–242.

Appendix A

Individual Characteristics of Each of the Six Groups of Neurons

TABLE A1. Morphological characteristics of Group 1 neurons.

Layer II pyramidal neurons with bifurcating apical dendrite

		Perimeter(µm)	Area(µm²)	Feret Max(µm)	Feret Min(µm)	Aspect Ratio
SOMATIC VARIABLES	avg/std	55.2 (5.9)	202.7 (31.3)	19.8 (2.4)	13.6 (1.0)	1.5 (0.2)

DENDRITIC CHARACTER		Qty	Nodes	Length(µm)	mean len	Surface(µm²)	mean sur	Volume(µm³)	mean vol
APICAL DENDRITE	avg / std	---	12.9 (6.7)	1278.7 (592.4)	---	5050.7 (2288.0)	---	2073.4 (995.4)	---
BASILAR DENDRITES	avg / std	3.1 (1.2)	11.4 (7.5)	1033.0 (516.3)	344.9 (136.6)	3085.5 (1421.3)	1026.4 (375.3)	918.9 (453.7)	303.5 (126.0)

MAX. HORIZ. SPREAD		Medial (µm)	Lateral (µm)	Total (µm)
APICAL DENDRITE	avg / std	95.9 (46.5)	112.6 (41.8)	207.4 (71.6)
BASILAR DENDRITE	avg / std	93.0 (32.5)	108.5 (52.6)	201.6 (61.7)

DISTANCE FROM SOMA TO FIRST APICAL BRANCH POINT (µm)
21.9 (14.4)

TABLE A2. Morphological characteristic of Group 2 neurons.

Layer II pyramidal neurons with nonbifurcating apical dendrite

		Perimeter(μm)	Area(μm²)	Feret Max(μm)	Feret Min(μm)	Aspect Ratio
SOMATIC VARIABLES	avg/std	52.1 (5.5)	183.1 (35.8)	18.7 (2.5)	13.3 (1.4)	1.4 (0.1)

DENDRITIC CHARACTER		Qty	Nodes	Length(μm)	mean len	Surface(μm²)	mean sur	Volume(μm³)	mean vol
APICAL DENDRITE	avg / std	---	9.6 (3.3)	1041.2 (362.4)	---	3735.4 (1236.6)	---	1404.1 (482.5)	---
BASILAR DENDRITES	avg / std	2.7 (0.8)	11.3 (3.7)	1093.4 (298.8)	426.6 (158.3)	3200.4 (936.7)	1248.9 (461.9)	975.0 (417.9)	380.1 (184.4)

MAX. HORIZ. SPREAD		Medial (μm)	Lateral (μm)	Total (μm)
APICAL DENDRITE	avg / std	92.9 (19.2)	90.5 (40.1)	183.5 (47.1)
BASILAR DENDRITE	avg / std	102.6 (16.3)	148.3 (59.0)	250.9 (68.7)

DISTANCE FROM SOMA TO FIRST APICAL BRANCH POINT (μm)
25.7 (10.0)

TABLE A3. Morphological characteristics of Group 3 neurons.

Layer III pyramidal neurons

		Perimeter(µm)	Area(µm²)	Feret Max(µm)	Feret Min(µm)	Aspect Ratio
SOMATIC VARIABLES	avg/std	56.1 (7.5)	200.8 (41.8)	18.5 (2.1)	14.5 (1.7)	1.3 (0.1)

DENDRITIC CHARACTER		Qty	Nodes	Length(µm)	mean len	Surface(µm²)	mean sur	Volume(µm³)	mean vol
APICAL DENDRITE	avg / std	---	9.2 (4.2)	884.0 (399.3)	---	3319.6 (1709.5)	---	1435.0 (902.1)	---
BASILAR DENDRITES	avg / std	4.0 (1.2)	11.2 (5.4)	1045.4 (596.7)	261.3 (129.3)	3155.3 (1825.2)	776.8 (349.8)	997.8 (648.1)	244.0 (123.7)

MAX. HORIZ. SPREAD		Medial (µm)	Lateral (µm)	Total (µm)
APICAL DENDRITE	avg / std	89.5 (59.0)	86.3 (39.8)	175.7 (80.6)
BASILAR DENDRITE	avg / std	121.2 (59.3)	107.6 (50.2)	228.8 (86.9)

DISTANCE FROM SOMA TO FIRST APICAL BRANCH POINT (µm)
26.4 (23.1)

TABLE A4. Morphological characteristics of Group 4 neurons.

Layer V-VI pyramidal neurons

		Perimeter(µm)	Area(µm²)	Feret Max(µm)	Feret Min(µm)	Aspect Ratio
SOMATIC VARIABLES	avg/std	56.1 (5.9)	206.9 (34.1)	19.8 (3.0)	14.5 (0.8)	1.4 (0.2)

DENDRITIC CHARACTER		Qty	Nodes	Length(µm)	mean len	Surface(µm²)	mean sur	Volume(µm³)	mean vol
APICAL DENDRITE	avg / std	---	9.8 (3.2)	1038.1 (429.0)	---	3217.0 (1163.4)	---	1065.1 (373.1)	---
BASILAR DENDRITES	avg / std	3.8 (1.7)	10.9 (7.3)	1011.8 (655.9)	258.8 (157.5)	3116.8 (1752.7)	807.9 (391.6)	948.8 (484.5)	250.9 (111.4)

MAX. HORIZ. SPREAD		Medial (µm)	Lateral (µm)	Total (µm)
APICAL DENDRITE	avg / std	115.8 (120.6)	95.1 (34.5)	211.0 (131.6)
BASILAR DENDRITE	avg / std	109.2 (44.6)	117.4 (48.9)	226.6 (88.8)

DISTANCE FROM SOMA TO FIRST APICAL BRANCH POINT (µm)
10.5 (6.1)

TABLE A5. Morphological characteristics of Group 5 nonpyramidal neurons.

Layer II-III nonpyramidal neurons									
		Perimeter(µm)	Area(µm²)	Feret Max(µm)	Feret Min(µm)	Aspect Ratio			
SOMATIC VARIABLES	avg/std	51.8 (14.5)	160.0 (38.7)	17.0 (2.9)	12.5 (1.9)	1.4 (0.2)			
		Qty	Nodes	Length(µm)	mean len	Surface(µm²)	mean sur	Volume(µm³)	mean vol
DENDRITIC CHARACTER	avg / std	3.8 (1.6)	11.8 (7.5)	1109.3 (721.9)	303.2 (180.7)	3281.0 (2341.6)	918.0 (686.3)	1027.3 (862.7)	293.2 (277.0)
		Medial (µm)	Lateral (µm)	Total (µm)					
MAX. HORIZ. SPREAD	avg / std	81.8 (46.7)	90.6 (36.9)	172.4 (51.6)					

TABLE A6. Morphological characteristics of Group 6 nonpyramidal neurons.

Layer V-VI nonpyramidal neurons									
		Perimeter(µm)	Area(µm²)	Feret Max(µm)	Feret Min(µm)	Aspect Ratio			
SOMATIC VARIABLES	avg/std	55.7 (8.7)	202.3 (58.2)	19.7 (3.5)	13.5 (2.0)	1.5 (0.3)			
		Qty	Nodes	Length(µm)	mean len	Surface(µm²)	mean sur	Volume(µm³)	mean vol
DENDRITIC CHARACTER	avg / std	3.9 (1.6)	13.9 (6.3)	1345.4 (630.0)	373.6 (208.4)	5038.6 (2944.9)	1420.9 (1151.0)	2099.0 (1710.7)	619.2 (775.6)
		Medial (µm)	Lateral (µm)	Total (µm)					
MAX. HORIZ. SPREAD	avg / std	108.2 (48.7)	139.0 (47.1)	247.2 (153.4)					

Appendix B

The Six Groups of Neurons Identified

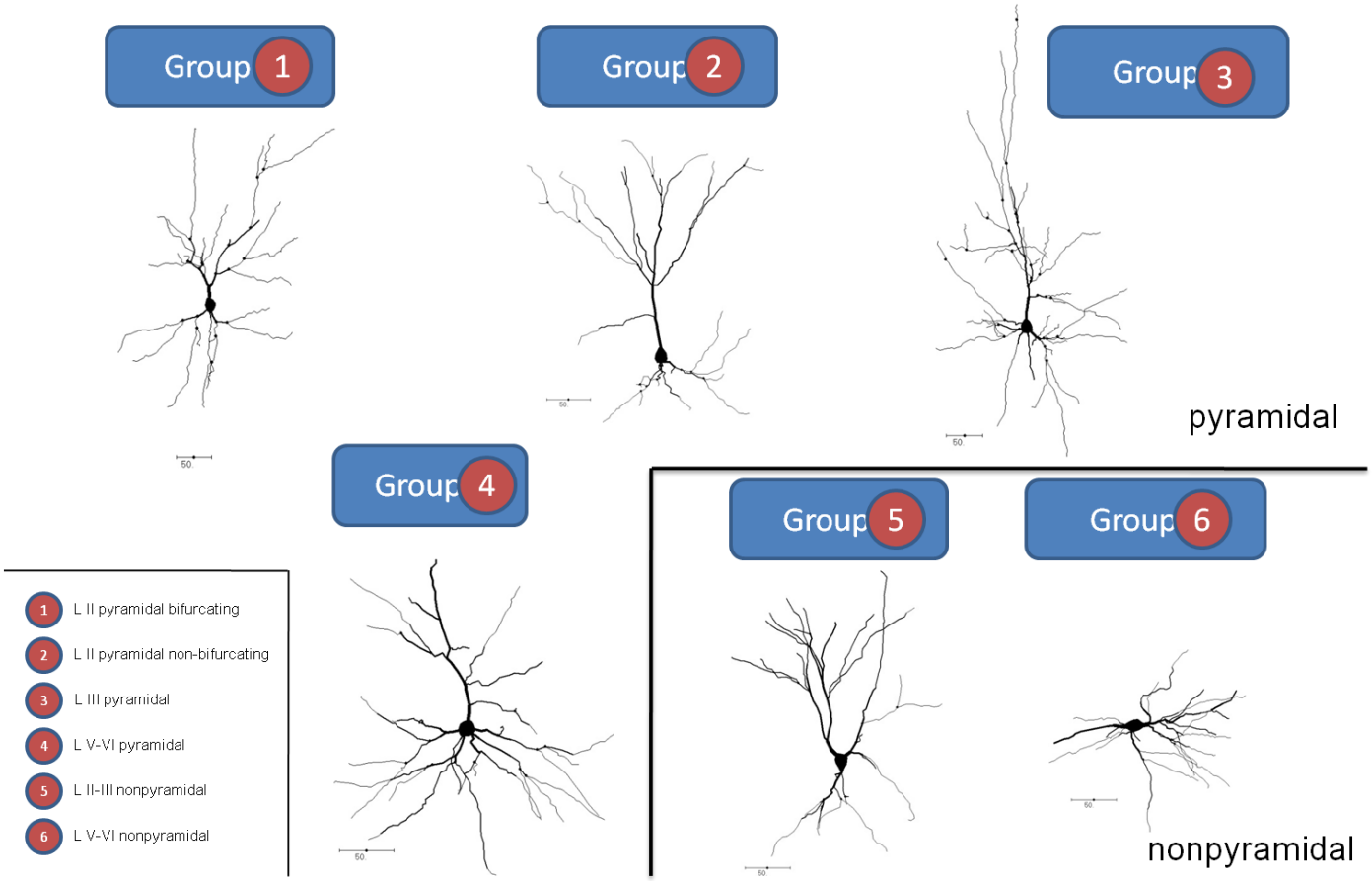

Figure 28. The six groups of neurons identified

Vita

Alexandru Ioan Cojanu was born on June 6th, 1985 in Bucharest, Romania and is an American citizen. After graduating from Miramar High School in Miramar, Florida, Alexandru pursued his undergraduate studies at The College of William and Mary in Willimamsburg, Virginia, receiving a Bachelor of Science degree in Kinesiology. Following a brief, year-long career as a Touring Professional Tennis Player during which he won three Professional-level doubles titles and reached a career-high ATP ranking of 512 in the world, he decided to pursue graduate studies at the Medical College of Virginia at Virginia Commonwealth University in Richmond, Virginia. There, he first received a Post-Baccalaureate Graduate Certificate in Pre-Medical Basic Health Sciences in May of 2010, and has spent the last year pursing his Master's degree in the Anatomy and Neurobiology Department. Alexandru will continue his studies pursuing a career as a physician in the coming years.